

ADDIS ABABA UNIVERSITY
SCHOOL OF GRADUATE STUDIES
DEPARTMENT OF CHEMISTRY



Master's Thesis (Chem.750)

**Optical and Metal Ion Sensing Properties of Electronically
Conducting Monomers and Polymer**

By

Wassie Mersha Takele

Advisor: Shimelis Admassie (PhD)

In Partial Fulfillment of the Requirements for Master of Science Degree in Chemistry
(Physical Chemistry)

June 2011

**Optical and Metal Ion Sensing Properties of Electronically
Conducting Monomers and Polymer**

By

Wassie Mersha

Approved by Examining Board:

Signature

Dr. Shimelis Admassie

Advisor

Professor Theodros Solomon

Examiner

Acknowledgments

First of all, I would like to thank almighty God who has been supported me throughout my life.

It is really difficult to list all individuals who kindly helped me during the journey towards my master's degree. I would like to acknowledge my advisor Dr. Shimelis Admassie for his unforgettable support and positive response to my questions during the main work. In addition, he devoted his time for correcting and editing of my whole paper up to the end of the work. I would like also to thank Ato Maereg Amare for being my co-advisor during this work and the contribution of him during all experimental works is remarkable. I am also thankful to Ato Solomon Mihretie for useful discussions throughout the work. Moreover, I want to acknowledge Prof. Wondimagegn Mammo and Ato Birhanu Wondimu for their contribution of polymer and monomers important for this work, respectively. I have also great appreciation to my friend Angaw Kelemwork for his memorable contribution of very important material to my thesis. In addition, I would like to thank Yemiker Mersha, Tizibt Amide, Meri Kibret, Tilahun Awok, and all my friends for different supports I gained from them.

Finally, I would like to give special thanks to Arba Minch University for the financial supports covered it to me. Moreover, I want to thank Chemistry department of Addis Ababa University for the contribution of all chemicals and instruments important for this work.

Table of Contents

	Page No.
Acknowledgment	i
Table of contents	ii
List of Figures	iv
List of Tables	vi
List of Abrivations and symbols	vii
List of Appendices	ix
Abstract	x
1. Introduction	1
1.1. General aspects	1
1.2. Objectives of the study	3
2. Litratue Review	4
2.1. Chemical sensors.....	4
2.1.1. Recognition elements of chemical sensors.....	4
2.1.2. Transduction elements of chemical sensors.....	5
2.1.3. Types of chemical sensors.....	6
2.1.3.1. Optical sensors.....	6
2.1.3.2. Electrochemical sensors.....	6
2.2. Phenomena of fluorescence emission	7
2.2.1. Radative and non-radative transition between electronic states	7
2.2.2. Fluorescence life time and fluorescence quantum yield	9
2.2.2.1. Excited state life time.....	10
2.2.2.2. Fluorescence quantum yield	10
2.2.3. Emission and excitation spectra.....	10
2.3. Principles of fluorescence quenching	11
2.3.1. Types of fluorescence quenching.....	12

2.3.1.1. Dynamic or collisional quenching.....	12
2.3.1.2. Static quenching.....	12
2.3.2. Mechanism of analytical detection during fluorescence quenching.....	13
2.3.2.1. Photoinduced electron transfer.....	13
2.3.2.2. Electron energy transfer.....	13
2.4. Fluorescence Chemosensors using monomers and conjugated polymers	14
2.4.2. Fluorescence Molecular Sensor for metal ions	14
2.4.1.1. Working principles of chemical sensors	15
2.4.1.2. Fluorescence molecular sensor of cations based on small molecules.....	16
2.4.1.3. Fluorescence molecular sensor of cations using conjugated polymers	20
2.4.1.4. Solvent effect on fluorescence molecular sensor of cation.....	22
3. Experimental Part..	26
3.1. Chemicals.....	26
3.2. Solution preparation	26
3.3. Instrumentation and optical measurement	27
4 . Results and Discussion	28
4.1. Optical properties of M1 , M2 , and P1 in different solvents.....	28
4.1.1. Uv-vis spectra for M1 , M2 , and P1	28
4.1.2 Fluorescence spectra for M1 , M2 , and P1	30
4.2. Fluorescence metal ion sensing properties of M1 and M2 in different solvents.....	34
4.2.1. Metal ion sensing propeties of monomers in THF and dioxane	35
4.2.2. Metal ion sensing propeties of monomers in chloroform	37
4.2.3. Relative sensitivity and selectivity of monomers towards metal ions.....	39
4.2.4. Stern-volmer analysis for Fe ³⁺ ion.....	42
4.2.5. Detection limit for Fe ³⁺ ion.....	49
4.3. Fluorescence cation sensing propeties of P1 in different solvents	53
5. Conclusions.....	57
6. References	58
Appendice	

List of Figures

	Page No.
Figure 1. The structure and nomenclature of monomers used for sensing.....	2
Figure 2. The structure and nomenclature of polymer used for sensing.....	2
Figure 3. Schematic illustration of chemical sensor.....	5
Figure 4. The Jablonski diagram	8
Figure 5. Molecular orbital schematic for photoinduced electron transfer.....	13
Figure 6. Schematic illustration for stepwise electron exchange	14
Figure 7. Molecular structure of podand- type receptor containing two pyrene units.....	17
Figure 8. Chemical structure of 2,6-bis(2-hydroxybenzyl-2-hydroxyethylamino)methyl-4- methylphenol	18
Figure 9. Molecular structure of pyrene compound	19
Figure 10. Chemical structure of rhodamine (Rh3) type fluorescence chemosensor.....	19
Figure 11. Chemical structure of polyquinoline ether.....	20
Figure 12. Molecular structure of water soluble phosphate functionalized polyfluorene.....	21
Figure 13. Molecular structure of imidazole-functionalized polyfluorene derivatives polymer and model compound.....	22
Figure 14. Structure of polyfluorenes with phosphate group and model compounds.....	24
Figure 15. Structure of naphthalimide.....	25
Figure 16. Absorption spectra for M1 in different solvents.....	29
Figure 17. Absorption spectra for M2 in different solvents.....	29
Figure 18. Absorption spectra for P1 in different solvents.....	30
Figure 19. Fluorescence spectra for M1 in different solvents.....	31
Figure 20. Fluorescence spectra for M2 in different solvents.....	32
Figure 21. Fluorescence spectra for P1 in different solvents.....	33
Figure 22. Fluorescence spectra for M1 in THF upon addition of different metal ions.....	35
Figure 23. Fluorescence spectra for M2 in THF upon addition of different metal ions.....	36
Figure 24. Fluorescence spectra for M1 in chloroform upon addition of different metal ions.....	37

Figure 25. Fluorescence spectra for M2 in chloroform upon addition of different metal ions.....	38
Figure 26. Emission response for M1 in THF upon addition of metal ions.....	39
Figure 27. Emission response for M2 in THF upon addition of metal ions.....	40
Figure 28. Emission response for M1 in chloroform upon addition of metal ions.....	41
Figure 29. Emission response for M2 in chloroform upon addition of metal ions.....	41
Figure 30. Fluorescence spectra for M1 in THF upon addition of different concentration of ferric ions.....	43
Figure 31. Fluorescence spectra for M2 in THF upon addition of different concentration of ferric ions.....	44
Figure 32. Stern-Volmer plot for M1 in THF.....	45
Figure 33. Stern-Volmer plot for M2 in THF.....	45
Figure 34. Fluorescence spectra for M1 in chloroform upon addition of different concentration of ferric ions.....	46
Figure 35. Fluorescence spectra for M2 in chloroform upon addition of different concentration of ferric ions.....	47
Figure 36. Stern-Volmer plot for M1 in chloroform	48
Figure 37. Stern-Volmer plot for M2 in chloroform	48
Figure 38. Calibration curves for M1 in THF.....	50
Figure 39. Calibration curves for M2 in THF.....	51
Figure 40. Calibration curves for M1 in chloroform	52
Figure 41. Calibration curves for M2 in chloroform	52
Figure 42. Fluorescence spectra for polymer in toluene upon addition of different metal ions.....	54
Figure 43. Fluorescence emission response for P1 in toluene upon addition of different metal ions.....	55
Figure 44. Fluorescence spectra for P1 in chloroform upon addition of different metal ions.....	56

List of tables

	Page No.
Table 1. Comparison of sensing ability of poly fluoren derivates for Fe ³⁺ ion.....	24
Table 2. Optical data for M1 and M2	34
Table 3. Optical data for polymer P1	34
Table 4. Stern-Volmer values for M1 and M2	49
Table 5. Limit detection values for M1 and M2	53

List of Abbreviations and Symbols

Ap	Electron acceptor
Cp	Conjugated polymer
C	Concentration
DMF	N,N-Dimethylformamide
DMSO	Dimethyl sulfoxide
Dp	Electron donor
EE	Electron exchange
$E_T(30)$	molar electronic transition energies
FPNA	9, 9-bis (3'-phosphatepropyl)-2, 7-diphenylfluorene sodium salt
HOMO	Highest occupied molecular orbital
I	Fluorescence intensity after addition of quencher
IC	Internal conversation
ICT	Intramolecular charge transfer
I_0	Fluorescence intensity without quencher
ISC	Inter system crossing
K^s_r	Rate constant for deactivation process
K^s_{nr}	Rate constant for non-deactivation process
K_{sv}	Stern-Volumer constant
L	2,6-bis(2-hydroxybenzyl-2-hydroxyethylamino)methyl-4-methylphenol
LOD	Limit of detection
LUMO	Lowest occupied molecular process
m	Slope
M1	2-(4, 7-di (thiophen-2-yl)-1H-benzo[d]imidazol-2-yl) phenol
M2	2-(2-methoxyphenyl)-4, 7-di (thiophen-2-yl)-1H-benzo[d]imidazole
OMOPr	Oligo (1-methoxy pyrene)

P1	poly (2-(9,9-dioctyl-9H-fluoren-7-yl)thiophen-2-yl)-4-pentylthiazol 2-yl)-5-(thiophen-2-yl)-4-pentylthiazole).
[Q]	Concentration of the quencher
PET	Photoinduced electron transfer
PFPNA	poly (9,9-bis(3'-phosphatepropyl)fluorene-alt-1,4-phenylene) sodium salt
S ₀	Singlet ground state
S ₁	First electronic state
S ₂	Second electronic state
THF	Tetrahydrofuran
T1	Triplet state
UV-Vis	Ultra violet visible
τ_s	Life time for excited state S1
τ_r	Radiative life time
ϕ_f	Fluorescence quantum efficiency
λ_{em}	Emission wavelength
λ_{ex}	Excitation wavelength
μM	Micro Molar
μ_g	Ground state dipole moment
μ_e	Excited state dipole moment

List of Appendices

Appendix 1. Uv-vis spectra for monomers in chloroform.....	62
Appendix 2. Fluorescence spectra recorded for monomer M1 in dioxane upon exposure to different metal ions.....	62
Appendix 3. Fluorescence spectra for M2 in dioxane upon addition of different metal ions.....	63
Appendix 4. Fluorescence spectra recorded for polymer P1 in THF upon exposure to different ions.....	63
Appendix 5. Fluorescence spectra recorded for polymer P1 in dioxane upon exposure to different ions.....	64
Appendix 6. Solvent polarity parameters.....	64

Abstract

Herein, the optical metal ion sensing properties of monomers (**M1** and **M2**) containing imidazole group as molecular recognition units and conjugated polymer (**P1**) carrying thiophene and thiazole in their backbone were studied. Absorption and fluorescence emission spectra of the materials considered were not significantly changed in different solvents. Sensing ability of the monomers and the polymer solutions to metal ions was carried out using fluorescence spectrometer. Both monomers were highly selective and sensitive optical chemosensor only to Fe^{3+} ion in THF, chloroform, and dioxane. The sensing principle was based on fluorescence quenching by forming complex between Fe^{3+} and imidazole group in the monomers backbone. The limit of detection values (LOD) for **M1** and **M2** in THF were 1.386×10^{-5} mol/L and 3.902×10^{-6} mol/L, respectively. Moreover, LOD values for **M1** and **M2** in chloroform obtained were 1.315×10^{-5} mol/L and 3.707×10^{-5} mol/L, respectively. The sensitivity of the monomers towards Fe^{3+} ion was compared by calculating Stern-Volmer constant (Ksv). The Ksv values found for **M1** and **M2** in THF were $6.474 \times 10^2 \text{ M}^{-1}$ and $1.495 \times 10^3 \text{ M}^{-1}$, respectively, and in chloroform the Ksv values obtained for **M1** and **M2** were $3.928 \times 10^2 \text{ M}^{-1}$ and $5.535 \times 10^2 \text{ M}^{-1}$, respectively. Results obtained showed that monomer **M2** was more sensitive than **M1** towards Fe^{3+} in all solvents considered. The fluorescence spectra of conjugated polymer **P1** in THF, toluene, chloroform, and dioxane was insensitive to all metal ions considered.

Key words optical chemical sensor; molecular recognition; fluorescence quenching; Stern-Volmer constant.

1. Introduction

1.1. General aspect

Metal ions are great concern not only among chemist but also among the general population, who are affected with some of the disadvantages associated with them. Although some heavy metal ions play important roles in living systems, they are very toxic and hence capable of causing serious environmental and health problems. For example, ferric is essential ion to most organisms, and both its deficiency and overload can induce various disorders with iron trafficking, storage, and balance. The excess of iron, however, can induce various disorders including some neurodegenerative diseases such as Alzheimer's and Parkinson's disease which are related to iron accumulation in brain. In addition to biological importance developing methods to monitor ferric ions also require on environmental aspects since iron is typical metals responsible for corrosion. It is also well known that mercury, lead and cadmium are toxic for organisms, and early detection in the environment is popular [1, 2, and 3]. As a result in this technological era, thinking to develop cheaper and faster methods for determination of metal ions leads to the concept of optical chemical sensors.

Electronically conducting monomeric compounds are organic molecules of relatively low molecular mass. They represent the major class of luminophores from the view point of application and diversity of chemical structure and properties. A conducting polymer is a carbon-based macromolecule through which the valence π -electrons are delocalized. Before the idea of conducting polymers, organic monomers have been used as recognition unit to sense metal ions for long period of time. Recently, the interests of chemical scientist using conjugated polymers (CP) as active site to develop chemical sensors to study metal ions have increased. This is due to the conjugated structure of the conducting polymers are responsible for strong absorption and emission in the Uv-Vis range and emission intensity, emission maximum, etc of the CP are easily perturbed during titration with metal ions.

This work focuses to study the optical chemosensory properties of electronically conducting monomers and polymer towards different metal ions. Moreover, we also investigated the effect of different solvents on the fluorescence properties of the materials included in the study in the presence of different metal ions.

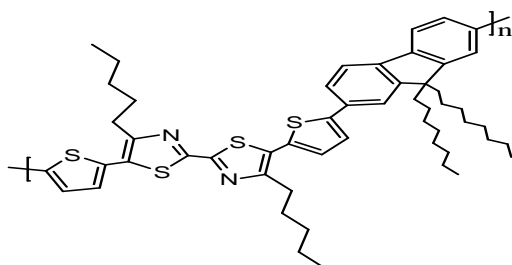
In this work the monomers used for sensing of cations contain heterocyclic imidazole derivatives (Figure 1) whose optical properties are changed upon interaction between imidazole and metal ions. The optical and fluorescence sensing properties of **P1** (Figure 2) in presence different metal ions was also investigated.



M1: 2-(4, 7-di (thiophen-2-yl)-1H-benzo[d]imidazol-2-yl) phenol and

M2: 2-(2-methoxyphenyl)-4, 7-di (thiophen-2-yl)-1H-benzo[d]imidazole

Figure 1. The structure and nomenclature of monomers used for sensing metal ion



P1: poly (2-(9,9-dioctyl-9H-fluoren-7-yl)thiophen-2-yl)-4-pentylthiazol-2-yl)-5-(thiophen-2-yl)-4-pentylthiazole).

Figure 2. The structure and nomenclature of polymer (**P1**) used for sensing metal ions.

1.2. Objectives of the study

A. General objective

The main objective of this work is to study the optical properties of electronically conducting monomers and polymer in presence of different metal ions.

B. Specific objectives

The specific objectives of the work include:

- (i) Identifying the metal cation (s) which quench or enhance the emission intensity of **M1**, **M2** and **P1**.
- (ii) Comparing the metal ion sensing ability of **M1**, **M2** and **P1** by calculating the Stern-Volmer constant, and
- (iii) Investigating the effect of solvents on the fluorescence sensing properties of **M1**, **M2** and **P1** towards different metal ions.

2. Literature Review

There is an enormous demand for chemical sensors for many areas and disciplines, especially in the area of Chemical and Biological sciences. High sensitivity and ease of operation are two main issues for sensor development. Fluorescence techniques can easily fulfill these requirements and therefore fluorescent-based sensors appear as one of the most promising candidates for chemical sensing of metal ions [4]. Hence, in this chapter theoretical backgrounds on chemical sensor and fluorescence emission phenomena are explained. In addition, different works conducted on sensing of metal ions using conjugated polymers and small molecules are also reviewed and illustrated with representative examples.

2.1. Chemical sensors

Chemical sensors are measurement devices that convert a chemical or physical property of a specific analyte into a measurable signal, whose magnitude is normally proportional to the concentration of the analyte. Generally, chemical sensing consists of two basic components connected in series such as a chemical (molecular) recognition system or receptors and transducers [4, 5].

2.1.1. Recognition elements of chemical sensors

Recognition elements are the key components of any chemical sensor. An ideal sensor is a device that will only detect a desired target analyte that is present within a given sample. Unfortunately, most samples usually contain many other analytes that may interfere with the sensor's ability to detect the target analyte. As a result it becomes necessary to design sensors which are as specific as possible for an analyte so that the sensor will discriminate against any interferences present. This is achieved using molecular recognition, where the sensor contains what is called a host molecule or chemoreceptor that will selectively bind the target analyte (which is quite often referred to as a guest).

One of the key requirements for molecular recognition is the existence of pre-organized groups within the host molecule that can selectively enclose or bind the guest ion (single atom) or molecule. In designing host molecules to be used in a sensor: the host molecule should be stable to the conditions in which it will be used, it must be able to selectively bind the target analyte in the sample, and it must be capable of being immobilized in a film/membrane which is contacted with the sample [5, 6].

2.1.2. Transduction elements of chemical sensors

Today signals are processed nearly exclusively by means of electrical instrumentation. Accordingly every sensor should include a transduction function, i.e. the actual concentration value, a non-electrical quantity must be transformed into an electrical quantity such as voltage, current or resistance. In chemical sensors this is done by transducers, which are a device that convert an observed change (physical or chemical) into measurable signal [7].

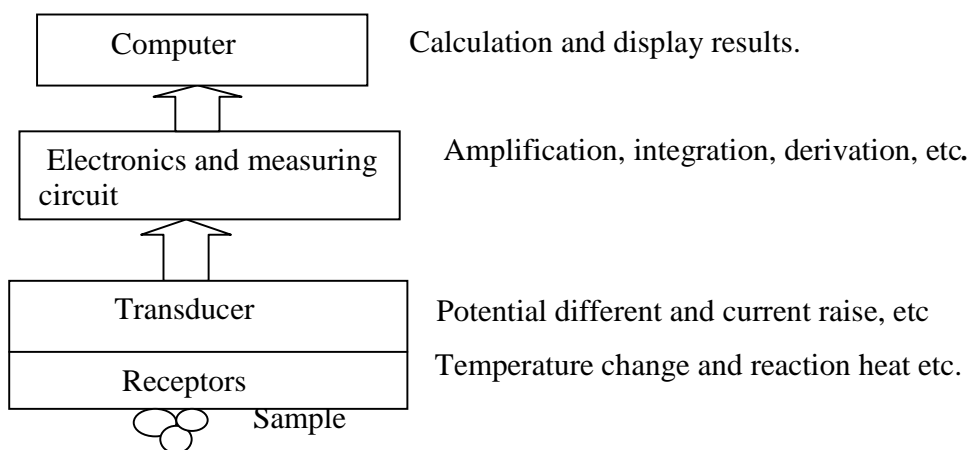


Figure 3. Diagram shows elements of chemical sensors [6].

2.1.3. Types of chemical sensors

On the basis of transduction principle, chemical sensors can be classified into three major classes with different transducers. Sensors with electrical transducer, sensors with optical transducer, and sensors with other transducer (e.g., mass change) [4]. However, chemical sensors based on optical change and electrochemical responses are common [8].

2.1.3.1. Optical sensors.

Optical sensor devices can be used for the detection and determination of physical or chemical parameters through the measurement of changes in some optical property. Most optical sensors are based on a spectroscopic technique such as measurement of absorbance, reflectance or fluorescence, where the signal obtained is related to the concentration of the analyte. The two most popular methods are absorption and fluorescence. If both modes of detection are available for a particular compound, fluorescence would be preferable because of better sensitivity due to being measured against an almost zero background [8, 9].

2.1.3.2. Electrochemical sensors

Electrochemical sensors are the largest and the oldest group of chemical sensors. They are divided by their mode of measurement into potentiometric (measurement of voltage at zero current), amperometric (measurement of current while potential is kept constant), conductimetric (measurement of conductivity change), and voltammetry (monitoring the change in current while by varying the applied potential) [4, 5].

2.2. Phenomena of fluorescence emission

Molecules absorb UV and visible radiation by undergoing electronic and vibrational excitation. Some of the absorbed energy is given off as heat to the solvent and some is emitted as radiation. In some unique chemical reactions radiation is emitted while a reaction is occurring. In general, the emitted radiation in these processes is called luminescence. The ways of energy release are divided into two categories; radiative and non-radiative transitions according as energy are released as light [9].

2.2.1. Radiative and non-radiative transitions between electronic states

Once a molecule is excited by absorption of a photon, it can return to the ground state with emission of fluorescence, but many other pathways for de - excitation are also possible. The categories of molecules capable of undergoing electronic transitions that ultimately result in fluorescence are known as fluorescence probes [10].

Jablonski diagram

The processes that occur in excited states after absorption of light is illustrated by Jablonski diagram. This diagram is named after Professor Alexander Jablonski, who is considered as the father of fluorescence spectroscopy. A typical Jablonski diagram is shown in Figure 4 below and it used to explain various molecular processes that occur in excited state. The singlet ground, first and second electronic states are denoted by S_0 , S_1 , S_2 , respectively. At each of these electronic energy levels the fluorophore can exist in a number of vibrational energy levels, depicted by 0, 1, 2, etc. and the triplet state is denoted by T_1 [9,10].

Absorption is very fast (1.0×10^{-15} s) processes and start from the 0 (lowest) vibrational energy level of S_0 because the majority of molecules are in this level at room temperature. Absorption of a photon can bring a molecule to one of the vibrational levels of S_1 , S_2 , etc. Following light

absorption several radiative and non-radiative processes occur for the excited molecules and these processes are detailed below [9].

Internal conversion(IC) is a non-radiative transition between two electronic states of the same spin multiplicity showed below by curved connector in Figure 4. A fluorophore is usually to some higher vibrational level of either S_1 or S_2 . With few exceptions molecules in condensed phase rapidly relax to the lowest vibrational level of S_1 . This process is called internal conversion(IC). From S_1 internal conversion to S_0 is possible but is less efficient than conversion from S_2 to S_1 , because of the much larger energy gap between S_1 and S_0 [9, 11].

Radiative transition with emission of photons from S_1 to S_0 is called fluorescence. It is common that apart from a few exceptions fluorescence emission occurs from S_1 electronic state. The 0 to 0 transition is usually the same for absorption and fluorescence, and an interesting consequence of this is emission spectrum is typically mirror image of absorption spectrum of the $S_0 \rightarrow S_1$ transition [11, 12].

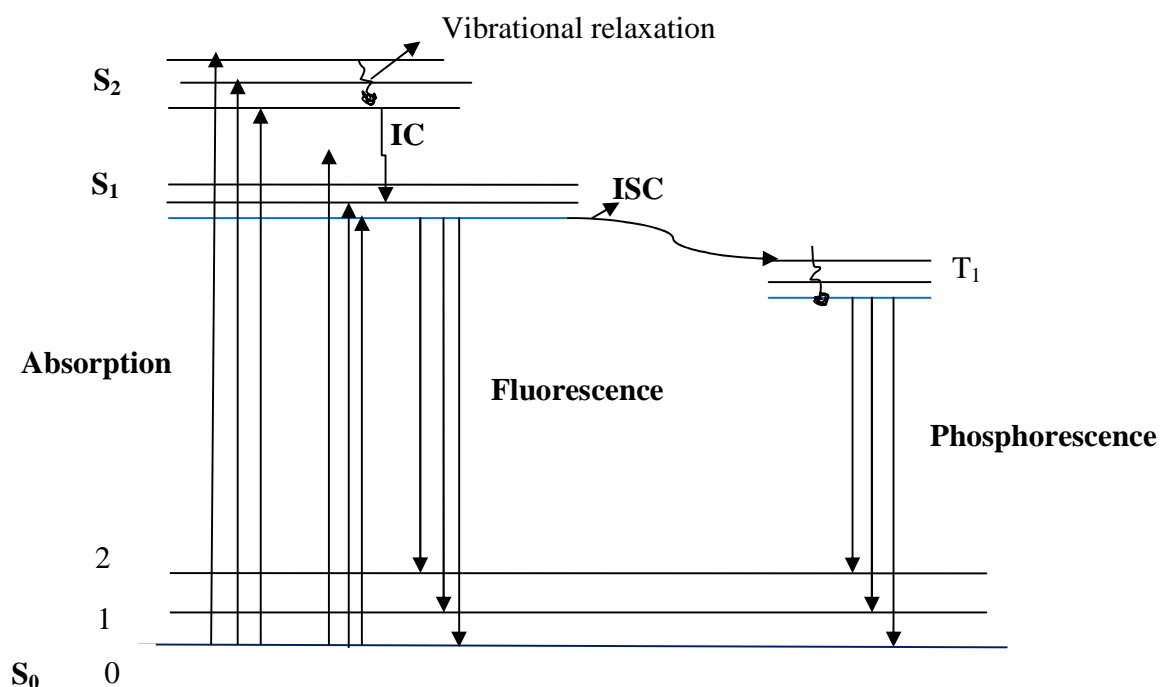


Figure 4. Jablonski Energy Diagram [9].

Examination of the Jablonski diagram shows that the energy of emission is typically less than that of absorption because of the energy loss in the excited state due to vibrational relaxation. So the fluorescence spectrum is located at higher wavelengths (lower energy) than the absorption spectrum. This phenomenon was first observed by Sir.G.G. Stokes in 1852. The gap (expressed in wave numbers) between the maximum of the first absorption band and the maximum of fluorescence is called the Stokes shift [9].

Intersystem crossing (ISC) is a non-radiative transition between two isoenergetic vibrational levels belonging to electronic states of different multiplicities. For example, an excited molecule in the 0 vibrational level of the S₁ state can move to the isoenergetic vibrational level of the T_n triplet state; then vibrational relaxation brings it into the lowest vibrational level of T₁. Crossing between states of different multiplicity is in principle forbidden, but spin-orbit coupling (i.e. coupling between the orbital magnetic moment and the spin magnetic moment) can be large enough to make it possible. It should also be noted that the presence of heavy atoms (i.e. whose atomic number is large, for example Br, Pb) increases spin-orbit coupling and thus favors intersystem crossing [13].

Emission from T₁ is termed phosphorescence, and is generally shifted to longer wavelength (lower energy) relative to fluorescence) because the energy of the lowest vibrational level of the triplet state T₁ is lower than that of the singlet state S₁ [10, 12].

2.2.2. Fluorescence lifetimes and quantum yields

The fluorescence lifetime and fluorescence quantum yield are perhaps the most important characteristics of a fluorophore. The life time of the excited state is defined by the average time the molecule spends in the excited state prior to return to the ground state. Quantum yield is the number of emitted photon relative to the number of absorbed photon [11].

2.2.2.1. Excited state lifetimes

If τ_s is the lifetime of excited state S_1 , it is given by

$$\tau_s = \frac{1}{K_r^s + K_{nr}^s} \quad (1)$$

Where k_r^s is rate constant for radiative deactivation $S_1 \rightarrow S_0$ with emission of fluorescence and k_{nr}^s is rate constant for non-radiative deactivation, i.e. sum of rate constant for internal conversion and rate constant for inter system crossing. If the only way of de-excitation from S_1 to S_0 was fluorescence emission, the lifetime would be $\frac{1}{K_r^s}$ this is called the radiative life time and denoted by τ_r [9, 10].

2.2.2.2. Fluorescence quantum yields

The quantum efficiency (ϕ_f) is an indication of the efficiency of the fluorescence process. A quantum efficiency of approximately 0.9 indicates a highly efficient process whereas $\phi_f = 0$ indicates that the molecule does not fluoresce. The fluorescence quantum yield ϕ_f is the fraction of excited molecules that return to the ground state S_0 with emission of fluorescence photons is given by:

$$\phi_f = \frac{K_r^s}{K_r^s + K_{nr}^s} = K_r^s \cdot \tau_s \quad (2)$$

Fluorescence quantum yield can be close to unity if the radiationless decay rate (K_{nr}^s) is much smaller than the rate of radiative decay (k_r^s) [9, 11].

2.2.3. Emission and Excitation spectra

For an ideal instrument, the directly recorded emission spectrum would represent the photon emission rate or power emitted at each wavelength, over a wavelength interval determined by the

slits widths and dispersion of the emission monochromator. If excitation wavelength (λ_{ex}) is held constant and the emission radiation is scanned, the resulting recording is called the emission spectrum. And an excitation spectrum is obtained by scanning excitation wavelength (λ_{ex}) and by holding constant the emission wavelength (λ_{em}) [11].

2.3. Principles of fluorescence quenching

Fluorescence intensity can decrease by variety of processes. Such decreases in intensity are called fluorescence quenching. A variety of molecular interaction result quenching includes excited state reactions, molecular-rearrangement, energy transfer, ground state complex formation and collision quenching. The Stern-Volmer relationship, named after Otto Stern and Max Volmer, allows us to explore the kinetics of a photophysical intermolecular deactivation process. The kinetics of fluorescence process follows the Stern-Volmer relationship, that is:

$$\frac{I_0}{I} = 1 + K_{sv}[Q] \quad (3)$$

Where I_0 is the intensity, or rate of fluorescence, without a quencher, I is the intensity, or rate of fluorescence, with a quencher, K_{sv} is stern-volmer constant and $[Q]$ is concentration of quencher. The constant K_{sv} determines the efficiency of quenching. When all other variables are held constant, the higher the K_{sv} , the lower the concentration of quencher required to quench the emission intensity. The value of K_{sv} is easily determined from the slope of the plot intensity change versus concentration of quencher. The dependence of the relative quantum yield of fluorescence has been calculated by the following equation [13, 14]:

$$\frac{\phi}{\phi_0} = \frac{1}{1 + K_s[Q]} \quad (4)$$

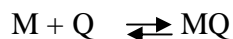
2.3.1. Types of fluorescence quenching

2.3.1.1. Dynamic (collisional) quenching

Dynamic quenching resulting from collisional encounter between the fluorophore and the quencher. In the case of collisional quenching, the quencher must diffuse the fluorophore during life time of the excited state and collisional quenching is time dependent processes. Upon contact the fluorophore return to the ground state, without emission of photon [9, 12].

2.3.1.2. Static quenching

Static quenching occurs as a result of formation of no fluorescence ground state complex between the fluorophore and the quencher. Let us consider the formation of a non-fluorescent 1:1 complex according to the equilibrium:



The excited-state lifetime of the uncomplexed fluorophore M is unaffected, in contrast to dynamic quenching. The fluorescence intensity of the solution decreases upon addition of Q, but the fluorescence decay after pulse excitation is unaffected.

The measurement of fluorescence life time is one of the important methods to distinguish static and dynamic quenching. There is no change in excited-state lifetime for static quenching, whereas in the case of dynamic quenching life time has been changed. One additional method to distinguish static and dynamic quenching is careful examination of the absorption spectra of the fluorophore. Collisional quenching only affects the excited state of the fluorophore, and thus no changes in absorption spectra are expected. In contrast ground state complex formation will frequently results in perturbation of absorption spectrum of the fluorophore [9,13].

2.3.2. Mechanism of analytical detection during fluorescence quenching

Photoinduced electron transfer and electron energy transfer (EET) are the major types of mechanisms in fluorescence quenching.

2.3.2.1. Photoinduced electron transfer (PET)

In photoinduced electron transfer complex is formed between the electron donor (D_P) and electron acceptor (A_P) yielding, $D_P^+ A_P^-$ (Figure 5). The subscript p indicates quenching is due to PET mechanism. This charge transfer complex can return to the ground state without emission of photon. Finally, the extra electron on the acceptor is return to the electron donor [9].

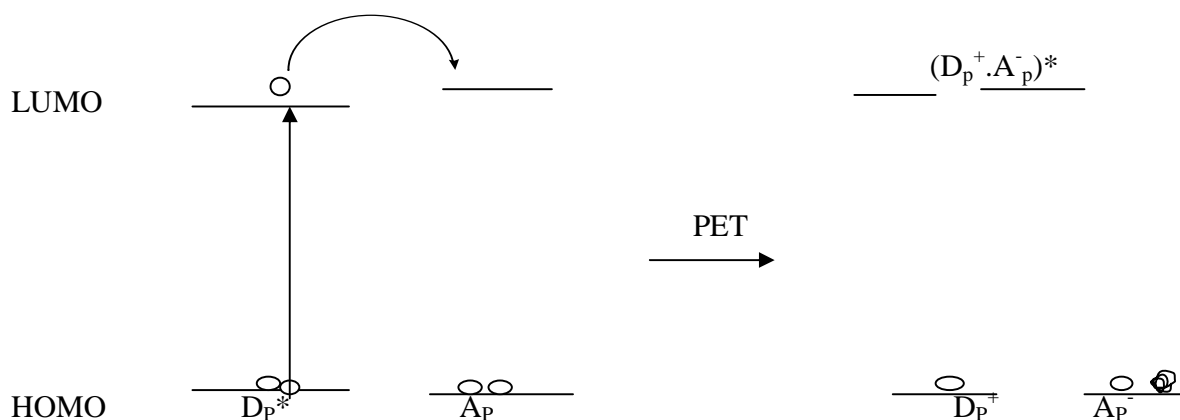


Figure 5. Molecular orbital schematic for PET [9].

2.3.2.2. Electron energy transfer (EET)

Electron energy transfer is another mechanism for the fluorescence quenching upon binding cations. EET or Dexter interaction occurs between donor D_E and acceptor A_E , where E indicates electron exchange. The excited donor has an electron in LUMO orbital. This electron is transfer to the acceptor. The acceptor transfers an electron again from its HOMO level, so the acceptor is

left in an excited state. The Dexter energy transfer requires close contact between the fluorophore and the cation and also direct orbital overlap [9, 41].

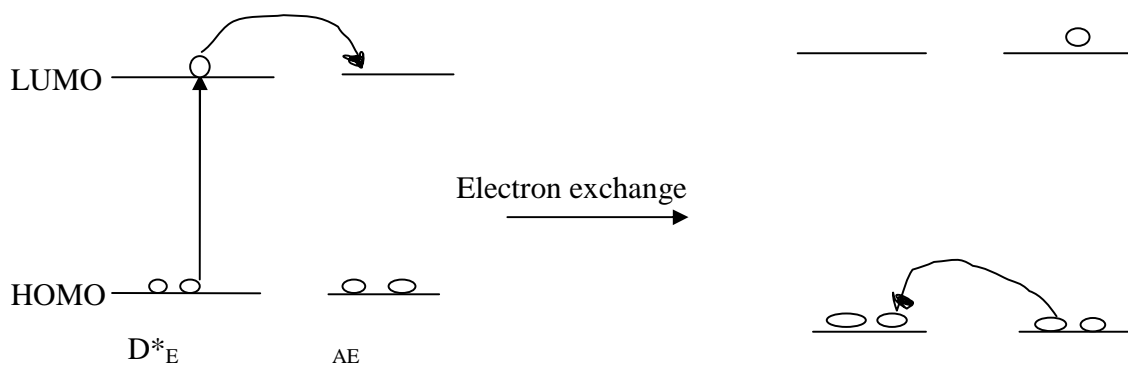


Figure 6. Schematic for stepwise electron exchange [adapted from ref. 9].

2.4. Fluorescence chemosensor using monomers and conducting polymers

There is a big need of selective and sensitive sensors for the detection of heavy metal ions in chemical and biological sciences. Optical chemical sensors are now become very important research topic and many efforts has been devoted to the design and synthesis of chemosensory systems that have the ability to detect metal ions and respond in terms of optical signals in real time. Among the systems reported to sense metal cations using crown ethers or their analogues are very common. Recently, much interest focused on conjugated polymers containing molecular recognition sites [15-27].

2.4.1. Fluorescent molecular sensors for metal ion

Chemosensors based on fluorescence signal changes are commonly referred as fluorescence chemosensors. The readout of fluorescent chemosensor is usually measured as change in fluorescent intensity, intensity decay life and shift of emission wavelength. An important feature of fluorescence chemosensor is that signal transduction of analytes binding event into the readout can happen in very short time and without any other assistance [15].

Fluorescence chemosensors for cations consists of two parts: ionophores and fluorophores. Ionophores are responsible for selective recognition of cations and fluorophore immediately converts the recognition event into optical signal by means of different photophysical processes. The choice of recognition moiety is of the utmost importance since it is responsible for the selectivity and the binding efficiency. The fluorophore acts as a signaling moiety since it converts the recognition event into an optical signal via the perturbation of various photoinduced processes such as electron transfer, charge transfer, excimer formation or energy transfer upon cation complexation [20].

2.4.1.1. Working principles of chemical sensors.

The general working principle of chemosensors is based on coordination events. The coordination of aromatic ligands by metal ions is an acid base reaction, in which the metal act as a Lewis acid (electron pair acceptor) and the ligand acting as the Lewis base (electron pair donor). As a result of this reaction there may be change of fluorescence spectra of the ligand when it interacts with cations [20]. Successful, selective receptor-analyte complex formation depends on size, shape and binding energy of the receptor and analyte molecules. In ion recognition complex selectivity (i.e. the preferred complexation of certain cation when other cation present) is of major important. In this regard the characteristics the ionophore that is the ligand topology and the number and the nature of complexing heteroatom or group should mach the characteristics of the cation that is radius, charge, coordination number. The stability of metal complex formed increase with metal ion charge/radii ratio. Another principle generally applicable in chemistry predicts that hard oxygen center combine with hard alkaline metal ions and soft sulfur or nitrogen center combine with soft transition metals. In addition, medium effect plays a great role on both selectivity and stabilities of complexation with cations. The main factors are: the difference between ligand coordination energy and solvation energy, that is, solvation power of the ligand as compared to that of the solvent and the difference of interaction with the ligand shell and dielectric medium outside the first solvation shell [15, 41].

2.4.1.2. Fluorescence molecular sensor of metal ions based on small molecules.

Small molecules as fluorescence sensors have extensively studied in the past several decades. The most commonly used fluorophores are aromatic compounds, especially anthracene. Crown compounds are known as one of the most interesting and promising components of photosensitive system. The discovery of crown ethers and cryptand in the late 1960s opened up new possibilities for cation recognition with improvement of selectivity, especially for alkali metal ions for which there is a lack of selective chelators [11, 15]. Many literatures are reported for detection of cations based on small optical molecules and some are detailed below.

Arai et al. have studied Na^+ fluorescence sensor based on podand- type receptor connecting two pyrene units and diphenyl ether, Figure 7. Three monomers, i.e. two monomers having two pyrene units as fluorophore (compound **1** and compound **2**) and one monomer having only one pyrene unit (compound **3**) in chloroform were used to investigate the binding ability of these compounds towards alkali metals (Li^+ , Na^+ , K^+ , Rb^+ , and Cs^+) [28]. The fluorescence spectra study of chloroform solutions of these compounds by excitation at 360 nm showed that compound having one pyrene unit have only the monomer emission at 423 nm. On the other hand, both compounds having two pyrene groups showed two emission bands at 423 nm and 524 nm. The emissions at 524 nm of compounds **1** and **2** are excimer emissions based on the intramolecular interaction between the two pyrene units.

To observe the metal ion binding properties of receptors **1**, **2**, and **3** the authors investigated the fluorescence changes upon addition of metal ions to the monomers solution. The fluorescence changes in compounds **1** and **3** were only slightly observed with addition of the alkali metal ions. On the other hand, fluorescence intensities of compound **2** having two pyrene units were changed by the addition of Na^+ and K^+ . Especially, Na^+ displayed a significant enhancement of the pyrene monomer emission of compound **2**. Their study of fluorescence intensity change of compound **2** with various concentration of Na^+ showed that excimer emission at 524 nm of **2** gradually decreases and the intensity of the monomer emission at 423 nm of **2** dramatically

increased with increasing Na^+ concentrations ranging from 2 μM to 200 μM . However, there was no spectral intensity change for compound **1** which have two pyrene units and compound **3** which have one pyrene unit. Finally, the researcher conclude that compound **2** is an effective fluorescence sensor for Na^+ and this binding ability of compound **2** is due to the presence of oxygen atom at the diphenylether component in compound **2** [28].



Figure 7. Molecular structures of pyrene compounds used to sense Na^+ ; (a) Compound **1** when $\text{X}=\text{CH}_2$ and Compound **2** when $\text{X}=\text{O}$ and (b) compound **3**.

A group of Wang, X. in 2009 reported a phenol-based compartmental ligand as a potential chemosensor for zinc (II) cation. Lewis base, 2, 6-bis (2-hydroxybenzyl-2-hydroxyethylamino) methyl-4-methylphenol (**L**), was used for Zn^{2+} ion as fluorescence chemosensor compound. The fluorescence of **L** is remarkably enhanced by Zn^{2+} as compared with K^+ , Ca^{2+} , Mg^{2+} , Cu^{2+} , Pb^{2+} , Mn^{2+} , Fe^{3+} , Fe^{2+} , Co^{2+} , Cd^{2+} , and Ni^{2+} ions. The fluorescence enhancement is attributed to the complexation of Zn^{2+} with **L**, which interrupts the photoinduced electron transfer process and rigidifies the molecular skeleton of **L** [29].

Results showed that alkali metal cation K^+ and the alkaline earth metal cations Ca^{2+} and Mg^{2+} hardly interfere with the fluorescence of **L** at high concentration (5 mmol L^{-1}) due to their poor complexation with **L**. However, the metal cations Pb^{2+} , Mn^{2+} , Co^{2+} , Ni^{2+} , and especially Cu^{2+} , Fe^{3+} , and Fe^{2+} reduce the fluorescence of **L** at relatively low concentration (0.5 mmol L^{-1}), probably due to an electron or energy transfer between metal cation and **L**. However, Cd^{2+} that has the same d^{10} electronic configuration as Zn^{2+} , does not enhance the fluorescence of **L**. Finally, from these observations they conclude that **L** may selectively signal the presence of Zn^{2+} in methanol-water solution [29].

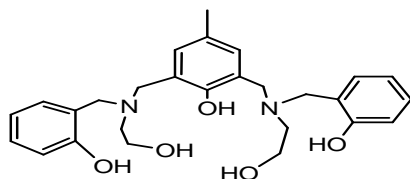
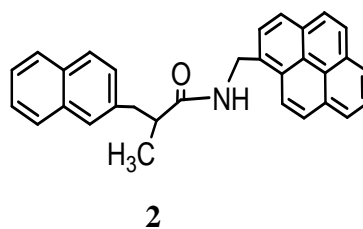
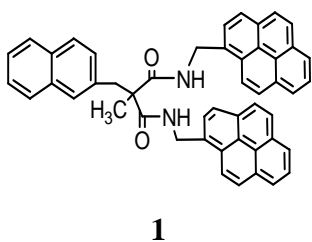


Figure 8. Structure of monomer **L** used to sense metal cations.

Kawakami, T et al. have investigated Cu^{2+} ion-selective fluoroionophore with dual off/on switches. New malonamide fluoroionophore possessing two pyrene moieties (derivative **1** and **3**) and one pyrene moieties (derivative **2**) were used as fluorescence unit. Fluorescence experiment result showed that bispyrenes **1** and **3** displayed both excimer and monomer emissions at 467 nm and 395 nm when excited at 344 nm in $\text{CH}_3\text{CN}/\text{CHCl}_3$ (9:1, v/v), respectively. Monopyrene **2** exhibited only typical monomer emission at 395 nm [30].

Fluorescence spectra experiment showed that addition of 1 equiv (1×10^{-5} M) of Ni^{2+} , Cu^{2+} , Zn^{2+} , and Ag^+ marginally affected the emissions of **1**. Interestingly, the results showed that monomer intensity was increase and excimer emission intensity was decrease by the addition of 10 equiv (1×10^{-4} M) of Cu^{2+} . They also found that the monomer and excimer emission intensities of derivative **3** were changed upon addition of 1 equiv (1×10^{-5} M) of Cu^{2+} selectively. Unlike bispyrene compounds, monopyrene **2** showed nonselective response to most of metal perchlorates. Finally, the researcher conclude that bispyrene **3** showed an excellent ion sensing ability to Cu^{2+} and bispyrene **1** displays the Cu^{2+} selective fluoroionophore with dual on/off switches by both monomer and excimer emissions. Such difference between bispyrenes **1** and **3** might result from the steric hindrance of the sp^3 carbon of malonamides affecting the intramolecular hydrogen bonds between both amide groups [30].



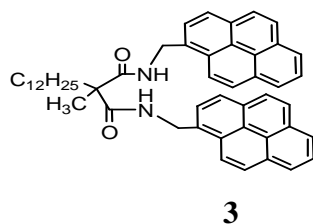


Figure 9 . Structure of pyrene compounds i.e. compound **1**, compound **2**, and compound **3**.

Gao et al. in 2010 developed Rhodamine (**Rh3**) based fluorescence chemosensor, which displays high selectivity for Fe^{3+} and shows wide detection range at different concentrations. Their results confirmed that the metal free **Rh3** was not showed any significant fluorescence emission in ethanol when the compound was excited at 525 nm, indicating that it exists as a non- fluorescent spirocyclic form in ethanol. Similarly addition of all tested metal ions (Ag^+ , Cd^{2+} , Cu^{2+} , Hg^{2+} , Mn^{2+} , Na^+ , Ni^{2+} , Pb^{2+} , and Zn^{2+}) cannot lead significant emission change except for Fe^{3+} . Upon addition of Fe^{3+} (10 equiv), **Rh3** displays strong fluorescence emission at 577 nm (205-fold).

Rh3 also exhibits negligible small fluorescence response to Pb^{2+} (13-fold). The fluorescence response of **Rh3** to Fe^{3+} ion is further studied by varying the concentration of Fe^{3+} ion from 0 to 160equiv. The fluorescence intensity is increased by 20-fold at 1.0 equiv and close to saturation at 160 equiv (800-fold). From this spectroscopic data the authors concluded that Rhodamine-based chemosensor **Rh3** shows high sensitivity and great selectivity toward Fe^{3+} ion over other metal ions [1].

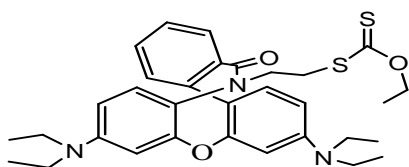


Figure 10. Chemical structure of **Rh3**

2.4.1.3. Fluorescence molecular sensor of metal ions using conjugated polymers

In 2001, Lee and coworkers have investigated polyquinoline ether and its optical properties in the presence of metal ions. The Polymer and the metal solutions used for fluorescence measurement were prepared in *N,N*-dimethylformamide/tetrahydrofuran (DMF/THF) (1:1 v/v) and water, respectively. Maximum fluorescence of the polymer solution was observed at 402 nm when the solution was excited at 356 nm. Among the metals under study, addition of Fe^{3+} , which is an electron-deficient metal cation, had a significant effect on the fluorescence intensity showing efficient quenching.

The degree of fluorescence quenching was clearly depending on the concentration of Fe^{3+} added. This research group pointed out that strong fluorescence quenching in the presence of Fe^{3+} and relatively little quenching in the case of Cu^{2+} or UO_2^{2+} may have resulted from an electron-transfer quenching effect by the more-oxidizing ferric ion center, which can be applicable to a photoinduced on-off switch. The Stern-Volmer constant values for Fe^{3+} , Cu^{2+} and UO_2^{2+} ions were $7.17 \times 10^3 \text{ M}^{-1}$, $3.25 \times 10^2 \text{ M}^{-1}$, and $3.07 \times 10^2 \text{ M}^{-1}$, respectively. Finally, from Stern-Volmer constant values they concluded that ferric ion shows 20 times more efficient fluorescence quenching than Cu^{2+} and UO_2^{2+} [32].

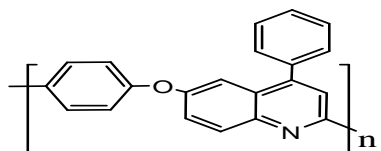


Figure 11. Chemical structure of polyquinoline ether used for sensing of ferric cation.

Wang et al. have been synthesized water soluble phosphate functionalized polyfluorene, i.e. poly (9,9-bis (3'-phosphatepropyl) fluorene-alt-1,4-phenylene) sodium salt (**PFPNa**) to be used as selective chemosensor for ferric cation. To investigate the photophysical properties absorption and fluorescence spectral of $1.0 \times 10^{-5} \text{ M}$ **PFPNa** and model monomer 9, 9-bis (3'-phosphatepropyl)-2, 7-diphenylfluorene sodium salt (**FPNa**) was measured in deionized water

Results revealed that absorption and fluorescence maxima were red shifted from 326 nm and 374 nm of model compound **FPNa** to 364 nm and 410 nm of polymer **PFPNa**, respectively due to increased conjugation of polymer backbone. Li^+ , K^+ , Mg^{2+} , Ca^{2+} , Sr^{2+} , Cd^{2+} , Mn^{2+} , Fe^{2+} , Cu^{2+} , Co^{2+} , Ni^{2+} , Zn^{2+} , Ag^+ , Hg^{2+} , Pb^{2+} , Fe^{3+} , and Al^{3+} cations were used to investigate the sensing properties of polymer **PFPNa**. Results obtained showed that the fluorescence spectrum of **PFPNa** was much more sensitive to Fe^{3+} over other cations. The Stern-Volmer constant was calculated at low concentration of ferric cation and the result was $1.84 \times 10^6 \text{M}^{-1}$ [32].

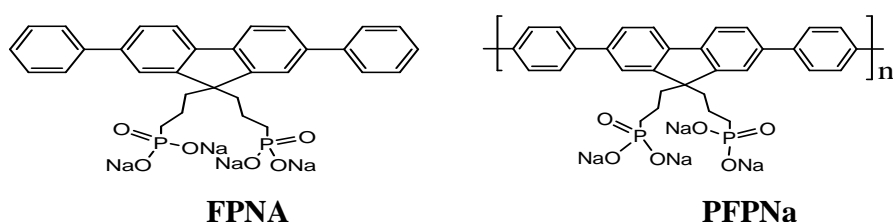


Figure 12. Molecular structure of **FPNa** and **PFPNa**

Zhou, X.-H. et al. have been developed an imidazole-functionalized polyfluorene derivatives as a chemosensory materials. They used $5 \mu\text{M}$ poly [(9,9-dihexylfluorene-2,7-diyl)-*alt-co*-(9,9-bis[6'-(1-imidazole-yl)hexyl]fluorene-2,7-diyl)] and its model compound (Figure 13) both diluted in THF to study sensing properties towards metal ions using Uv-vis absorption and photoluminescence spectra. Results obtained shows that the polymer had no response upon addition of alkali and alkali earth metal ions (up to 100ppm) for both absorption and fluorescence spectra due to poor coordination ability of the imidazole receptor with these metal ions. But among transition metals considered only Cu^{2+} was completely quench the emission intensity of the polymer. The sensing property of the polymer and the model monomer was compared using Cu^{2+} cation. They showed that the fluorescence intensity of the polymer was quenched more strongly in the presence of Cu^{2+} than the model compound. Calculated value of Stern-Volmer constant for the polymer and the model compound were $1.2 \times 10^7 \text{M}^{-1}$ and $1.1 \times 10^6 \text{M}^{-1}$, respectively [33].

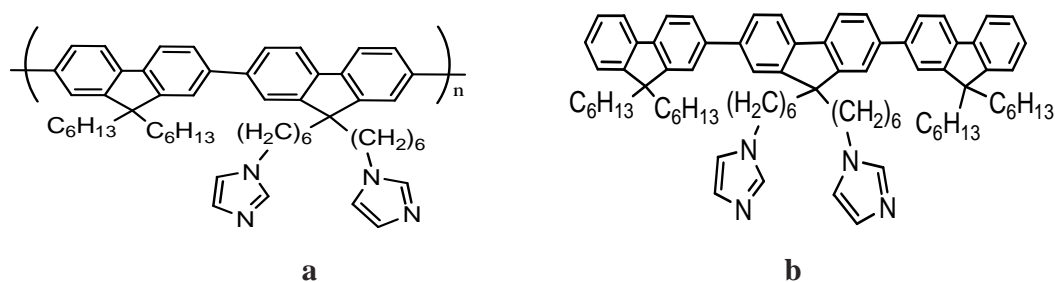


Figure 13. Molecular structure of imidazole-functionalized polyfluorene derivatives: **a)** polymer; **b)** model compound.

2.4.1.4. Solvent effects on fluorescence molecular chemical sensor.

Shifts in absorption and emission bands can be induced by a change in solvent nature or composition; these shifts, called solvatochromic shifts. In general, fluorophores with a large change in their permanent dipole moment upon excitation exhibit a strong solvatochromism. If the solute dipole moment increases during the electronic transition ($\mu_g < \mu_e$) a positive solvatochromism normally results. In the case of a decrease of the solute dipole moment upon excitation ($\mu_g > \mu_e$), a negative solvatochromism is usually observed [34-37].

In 2010, Geo, y. et al. studied the effect of side chain and solvent on the fluorescence spectra of highly fluorescence conjugated oligomer, Oligo (1-methoxy pyrene (OMOPr). The backbones of OMOPr contains alkoxy substitute and they explained that this substitute increase electron density of the material considered and unique optical properties were observed. In addition, they studied the effect of solvent polarity on the Uv-Vis and fluorescence spectra of OMOPr. Result obtained confirms that the Uv-Vis spectra of the oligomer were the same in all solvents considered and this indicates that the conformation of the OMOPr molecule is fixed due to high rotational energy barrier. However, the emission spectra of the material were solvent sensitive. As example, they compare for hexane and acetone and emission maximum obtained were 441 nm and 464 nm, respectively [35].

The work conducted by Lee J.K. and Lee T.S. investigated the optical properties of polybenzoxazole derivative with an adjacent hydroxyphenyl ring by adding various cations using different solvents. The metals under study were Mg^{2+} , K^+ , Ca^{2+} , UO_2^{2+} , and Fe^{3+} in DMF and methanol solvents for polymers dissolve in DMF and chloroform, respectively. The effects of metal cations on the emission intensity of the polymer in DMF and chloroform were investigated. Of the metal cations, magnesium cation led to large fluorescence enhancement, and ferric cation led to remarkable fluorescence quenching in DMF. For other metal cations, blue shifts of the emission were found with fluorescence quenching. Finally, they conclude that the polymer considered could be regarded as a probe material with a selective sensing ability towards DMF. On the other hand, the emission shift of the polymer was not affected by metal cations in chloroform, but significant fluorescence quenching was also induced upon exposure to ferric cation without large emission shift [38].

Wang et al. used polyfluorenes with phosphate group in the side chains as chemosensory and electroluminescence materials. According to results found the absorption and emission spectra of the materials used (**PF1** and **PF2**) are solvent dependent and showed red shift up to 14 nm and 16 nm, respectively, with increasing solvent polarity. The metal ions sensing properties of **PF1** and **PF2** were studied in different solvents (CH_2Cl_2 , THF, and ethanol). According to results obtained the polymers are sensitive and selective chemosensor for Fe^{3+} in all solvents among the metals considered. Their study showed that the emission intensity of **PF1** and **PF2** in CH_2Cl_2 solution was decreased significantly, that is 210-fold and 130-fold, respectively, upon addition of Fe^{3+} ion [39]. This quenching effect was due to the formation of certain complex between phosphate group in the polymers backbone and Fe^{3+} ion. Similarly the fluorescence intensity of **PF1** in THF was almost quenched after addition of $100 \mu\text{M}$ Fe^{3+} ion. However, when excess of Fe^{3+} ($100 \mu\text{M}$) was added into the ethanol solution of polymer **PF1** and **PF2**, the fluorescence intensity of **PF1** and **PF2** only drop 18-fold and 14-fold, respectively.

Table 1. Comparison of sensing ability of poly fluoren derivatives for Fe³⁺ ion.

	PF1		PF2	
	In CH ₂ Cl ₂	In ethanol	In CH ₂ Cl ₂	In ethanol
K _{sv} (M ⁻¹)	4.05x10 ⁶	3.55x10 ⁵	2.04x10 ⁶	2.71x10 ⁵

The difference sensitivity of **PF1** and **PF2** is probably due to the difference length of alkyl chains, which results difference distance between Fe³⁺- phosphate group quencher and polymer backbone. The decreasing quenching effect of **PF1** and **PF2** in ethanol solvent is due to hydrogen bonding interactions between the ethanol molecules and phosphate groups, which weaken the interaction between the receptor and the analyte [39].

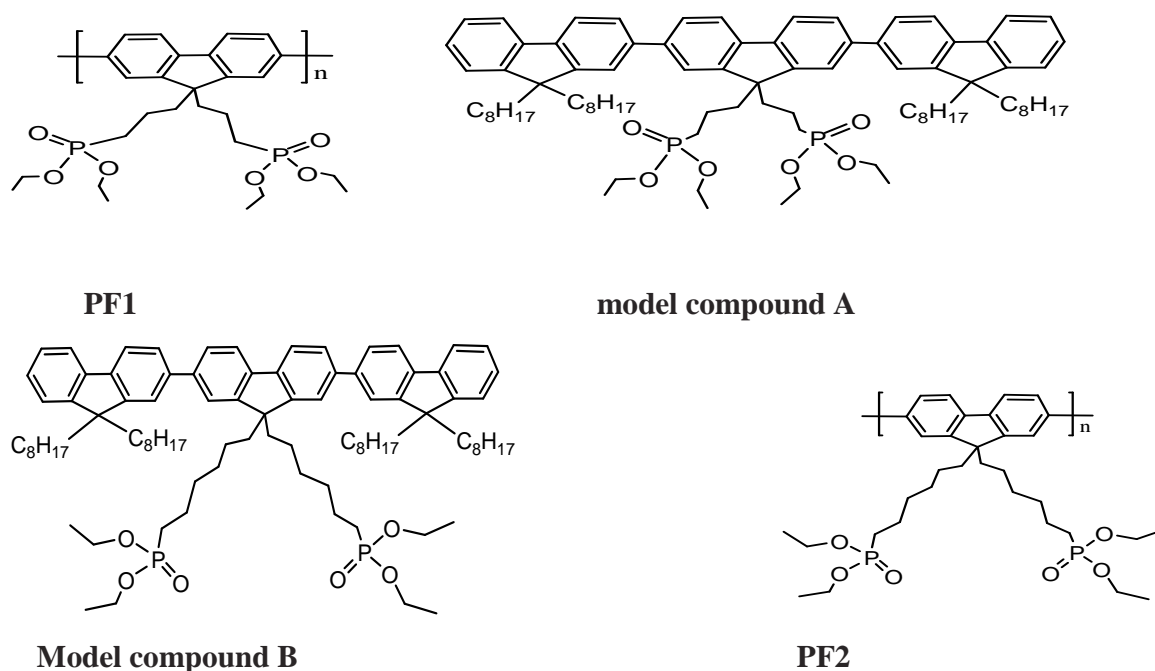


Figure 14. Structure of polyfluorenes with phosphate group and model compounds.

In 2007, the research group of Okamoto, H. have been studied the effect of solvent and metal cations on fluorescence spectra of modified naphthalimides **1** and **2** (Figure 15).

According to fluorescence spectra experiment the emission spectra of naphthalimides **1** produce violet fluorescence (λ_{fl} 388 nm) in MeCN and methanol. However, in DMSO an orange emission (λ_{fl} 575nm) was observed. Naphthalimide **2** displayed a blue fluorescence in MeCN (λ_{fl} 418 nm) and a yellow emission in DMSO (λ_{fl} 542 nm). The red-shifted emission observed for both in DMSO, which is stronger electron-pair donor (Lewis base), is thus attributed to the enhanced ICT (intramolecular charge transfer) character due to the formation of the amide-anion species. The fluorescence of the naphthalimide **2** in MeOH showed two emission bands (λ_{fl} 436 and 556 nm). It is probable that, in MeOH, both the amide **2** and its anion **2** - coexist in equilibrium, and due to these two species, the dual fluorescence was observed.

The metal cation sensing ability of naphthalimide **1** and naphthalimide **2** in acetonitrile and DMSO was also studied [38]. According to results obtained the naphthalimides were insensitive to metal cations in acetonitrile, while in DMSO the amide- anion bands were affected in presence of metal cations. The results obtained showed that for naphthalimide **1**, among the examined metal cations, the transition-metal cations effectively quenched the emission band: ten equivalents of Cu^{2+} almost completely quenched the fluorescence. Alkaline and alkaline-earth metal cations displayed slight to moderate quenching effects on the emission spectra of **1**. Naphthalimide **2** also responded to metal cations in DMSO. Concerning the emission spectra, Cu^{2+} reduced the fluorescence intensity up to 45%. Li^+ , Na^+ , Mg^{2+} and Ba^{2+} did not display any remarkable effects on the emission spectra of naphthalimide **2** [40].



Figure 15. (a) Structures of naphthalimides **1**; (b) Structure of naphthalimides **2**.

3. Experimental Part

3.1. Chemicals

The monomers (**M1** and **M2**) and the conjugated polymer (**P1**) used for optical and metal ion sensing study were synthesized and characterized by other researchers of chemistry department, Addis Ababa University (Ato Birhanu Wondimu and Professor Wondimagegn Mammo with his PhD student, respectively). The metal cations used in the study were in the form of nitrate salts, i.e., NaNO_3 (Riedel- de Haen, Germany), KNO_3 (Riedel - de Haen, Germany), $\text{Mg}(\text{NO}_3)_2 \cdot 6\text{H}_2\text{O}$ (Riedel- de Haen, Germany), $\text{Ca}(\text{NO}_3)_2 \cdot 4\text{H}_2\text{O}$ (Riedel- de Haen, Germany), $\text{Al}(\text{NO}_3)_3 \cdot \text{H}_2\text{O}$ (BDH Chemicals LTD, England), $\text{Cr}(\text{NO}_3)_3 \cdot 9\text{H}_2\text{O}$ (FIZMERK laboratory reagent), $\text{Fe}(\text{NO}_3)_3 \cdot 9\text{H}_2\text{O}$ (Riedel - de Haen, Germany), $\text{Co}(\text{NO}_3)_2 \cdot 6\text{H}_2\text{O}$ (FIZMERK laboratory reagent), $\text{Ni}(\text{NO}_3)_2 \cdot 6\text{H}_2\text{O}$ (Fluka, Switzerland), $\text{Cu}(\text{NO}_3)_2 \cdot 3\text{H}_2\text{O}$ (Fluka, Switzerland), $\text{Cd}(\text{NO}_3)_2 \cdot 4\text{H}_2\text{O}$ (Fluka, Switzerland), $\text{Zn}(\text{NO}_3)_2 \cdot 6\text{H}_2\text{O}$ (research – lab fine Chem industry, India), $\text{Cu}(\text{NO}_3)_2 \cdot 3\text{H}_2\text{O}$ (Nice chemicals Pvt.Ltd.), $\text{AgCl} \cdot 2\text{H}_2\text{O}$ (Aldrich) and HgCl_2 (Riedel- de Haen, Germany). The solvents used were chloroform (PHARMACOS LTD), methanol (SIGMA-ALDRICH), tetrahydrofuran (Lancaster synthesis), toluene (BDH Chemicals LTD, England), and dioxane (Scharlau). All chemicals were used as received from the store without further purification.

3.2. Solution preparation

The nitrate and chloride salts of the metal were dissolved in methanol solvent to prepare their corresponding 1.0×10^{-2} mol/L stock solutions. For ferric cation which showed proper fluorescence quenching different concentrations (8.0×10^{-3} , 6.0×10^{-3} , 1.0×10^{-3} , 8.0×10^{-4} , 2.0×10^{-4} , 6.0×10^{-5} , 1.0×10^{-5} , 8.0×10^{-6} , 1.0×10^{-6} mol/L in methanol) were prepared from the stock solution. 0.005 gm of **M1** and **M2** were dissolved in chloroform, THF, and dioxane to afford the stock solutions with concentration of 6.626×10^{-4} mol/L **M1** and 6.32×10^{-4} mol/L **M2**. With similar solvents these stock solutions were diluted to 6.626×10^{-6} mol/L **M1** and 6.32×10^{-6} mol/L **M2**.

Similarly 0.0025 gm of **P1** was dissolved in chloroform, Toluene, THF, and dioxane to afford the stock solution with concentration of 5.80×10^{-5} mol/L **P1**. Then this stock solution was diluted to 2.3×10^{-7} **P1** mol/L in chloroform, Toluene, THF, and dioxane. A monomer - metal mixtures used for fluorescence optical measurements were prepared by mixing 2 ml monomer solutions in solvents considered with 0.4 ml metal salts in methanol. Similarly, metal - polymer mixture was prepared by mixing 2 ml **P1** in solvents under the study with 0.4 ml metal salts in methanol.

3.3. Instrumentations and Optical measurements

The fluorescence emission spectra were record using Jobin Ivon Fluoromax-4 Spectrofluorometer. The Absorption spectra were also obtained using T60 UV-Vis spectrometer. Fluorescence emission spectra of 2.0 ml **M1** (6.626×10^{-6} mol/L) and 2.0 ml **M2** (6.32×10^{-6} mol/L) solutions in THF, chloroform, and dioxane were measured by exciting at 348 nm for chloroform and at 350 nm for THF and dioxane .The emission scan range for both monomers were adjusted from 360 nm to 600 nm. Similarly, emission spectra of polymer 2.0 ml **P1** (2.3×10^{-7} mol/L) in chloroform, THF, toluene and dioxine were recorded by exciting at 461 nm with emission scan from 470 nm to 800 nm. To study the metal responsive properties of **M1**, **M2**, and **P1** the emission spectra were recorded for the metal-monomer and metal - polymer solutions with the same experimental conditions as metal free monomers and polymer.

4. Results and Discussion

4.1. Optical properties of M1, M2, and P1 in different solvents.

The UV-Vis and fluorescence spectra of **M1**, **M2**, and **P1** were recorded in different solvents in order to study optical properties of monomers and polymer. The monomers and conjugated polymer used in this study were not easily soluble in more polar organic solvents (DMSO, methanol and DMF). Although **P1** was soluble in less polar toluene, **M1** and **M2** cannot dissolve in it. Of the tested solvents, only THF, chloroform, and dioxane were the common solvents.

4.1.1. Uv-Vis absorption spectra for M1, M2, and P1 in different solvents.

In order to determine the excitation wavelength and to investigate effect of solvent on absorption spectra of materials under study Uv-Vis spectra of **M1**, **M2**, and **P1** were studied. Figure 16 and 17 shows the UV-Vis spectra of **M1** and **M2** in THF and dioxane, respectively. **M1** and **M2** in THF and dioxane exhibit single absorption peak at 350 nm which may be due to $\pi \rightarrow \pi^*$ electronic transition of the monomers backbone. Similarly the absorption maximum of **M1** and **M2** in chloroform was observed at 348 nm, Appendix 1. As shown in Figure 18, **P1** in chloroform, toluene, THF, and dioxane shows absorption maximum at 458 nm. Due to effective conjugation length, the absorption peak of the polymer is more red shifted than the monomers [39].

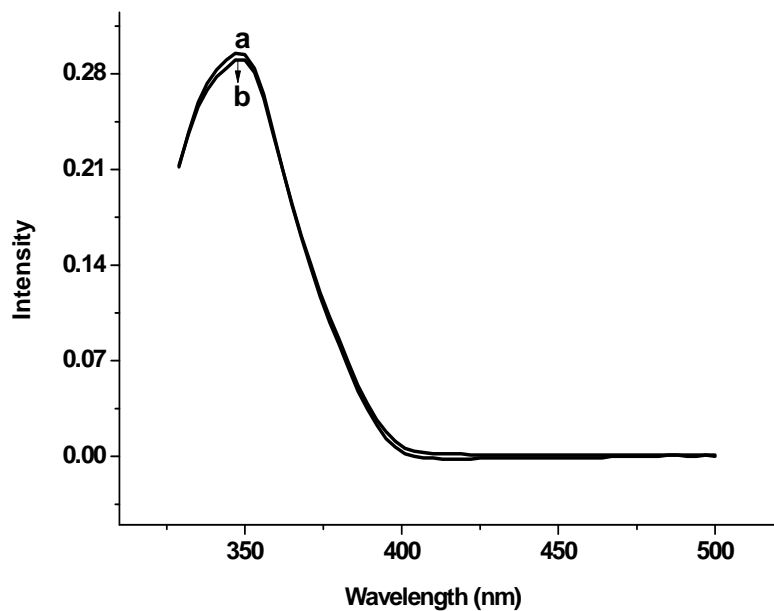


Figure 16. Absorption spectra recorded for **M1** (6.62×10^{-6} M) in (a. THF and b. dioxane).

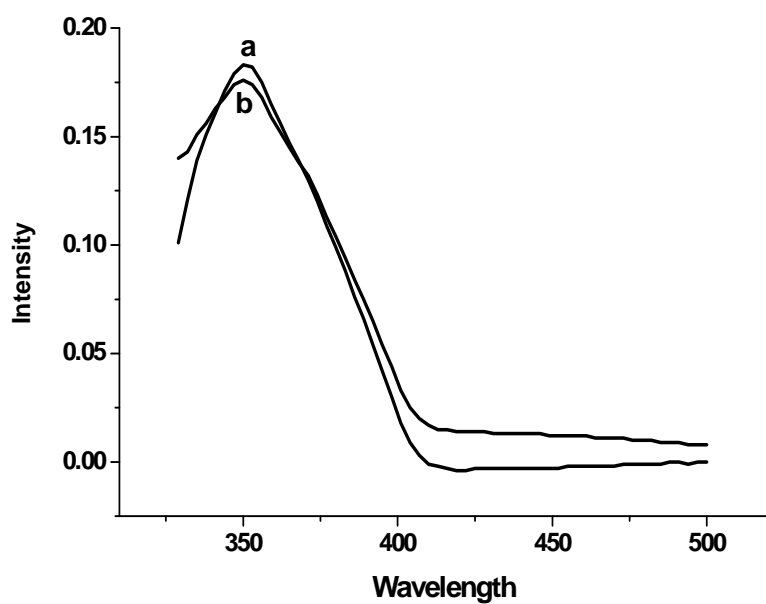


Figure 17. Absorption spectra recorded for **M2** (6.32×10^{-6} M) in (a. THF and b. dioxane).

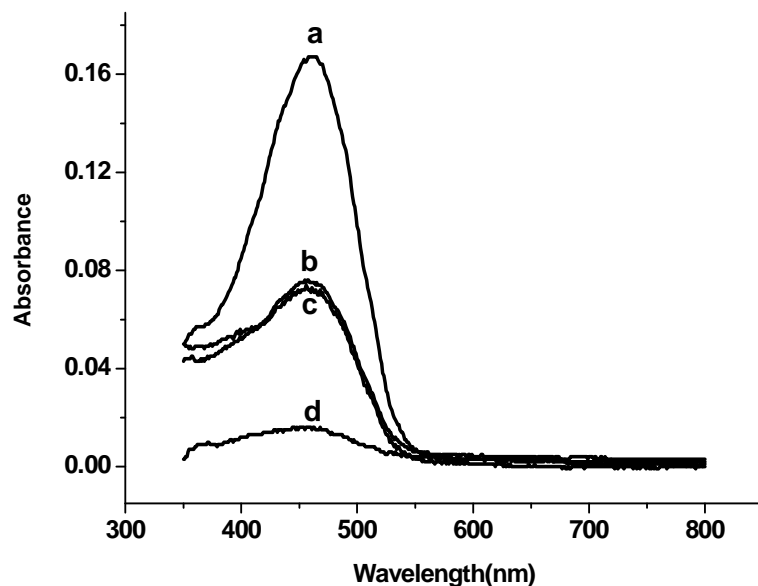


Figure 18. Absorption spectra recorded for **P1** ($2.3 \times 10^{-7} \text{M}$) in (a. chloroform, b. toluene, c. THF, and d. dioxane).

Similarities of the absorption spectra maximum of **M1** and **M2**, and identical absorption maximum of **P1** in the solvents under study may be resemblance of the monomer ground state structures in all solvents included [35]. Thus, results have shown that the absorption maxima of materials included in the study were not affected by solvent polarity.

4.1.2. Fluorescence emission spectra for **M1**, **M2**, and **P1** in different solvents.

To check the emission properties of materials considered (emission shape, emission intensity, and maximum emission wavelength) herein the fluorescence spectra were studied in different solvents. The emission spectra were recorded by exciting the samples at its maximum absorption wavelength. As shown in Figure 19, **M1** solution in THF and dioxane shows emission maxima at 420 nm and 418 nm with small shoulder around 476 nm, respectively.

However, the fluorescence maxima of **M1** in chloroform is peaked at 433 nm and the small shoulder observed in THF and dioxane around 476 nm becomes emission peak in the case of **M1** in chloroform. Dual emission peaks of **M1** in chloroform may be due to impurity or excimer formation i.e. intramolecular excimer emission because of strong π - π interaction between two fluorophore moieties [30, 47].

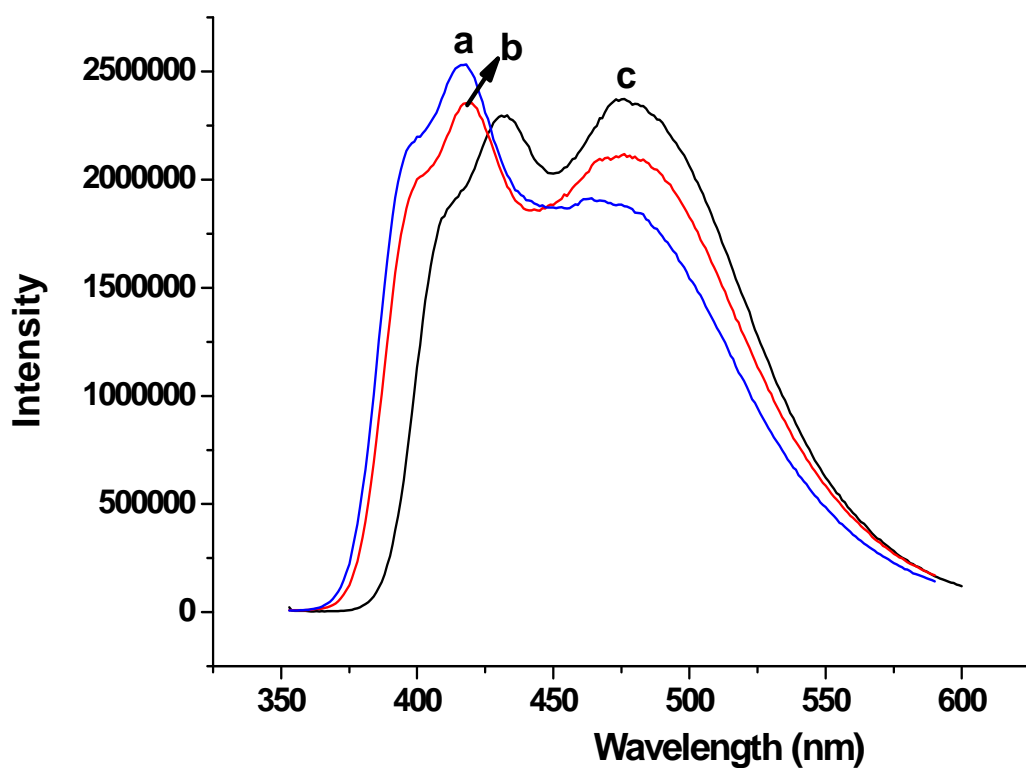


Figure 19. Fluorescence spectra recorded for monomer **M1** (a – c; in THF, dioxane, and chloroform. Concentration of **M1** was 6.62×10^{-6} M and excitation wavelength 350 nm for THF and dioxane and 348 nm for chloroform.

As shown in Figure 20, **M2** which has similar chemical structure with **M1** (only different in side chain) in dioxane, THF, and chloroform shows emission maximum at 423 nm, 425 nm, and 434 nm, respectively.

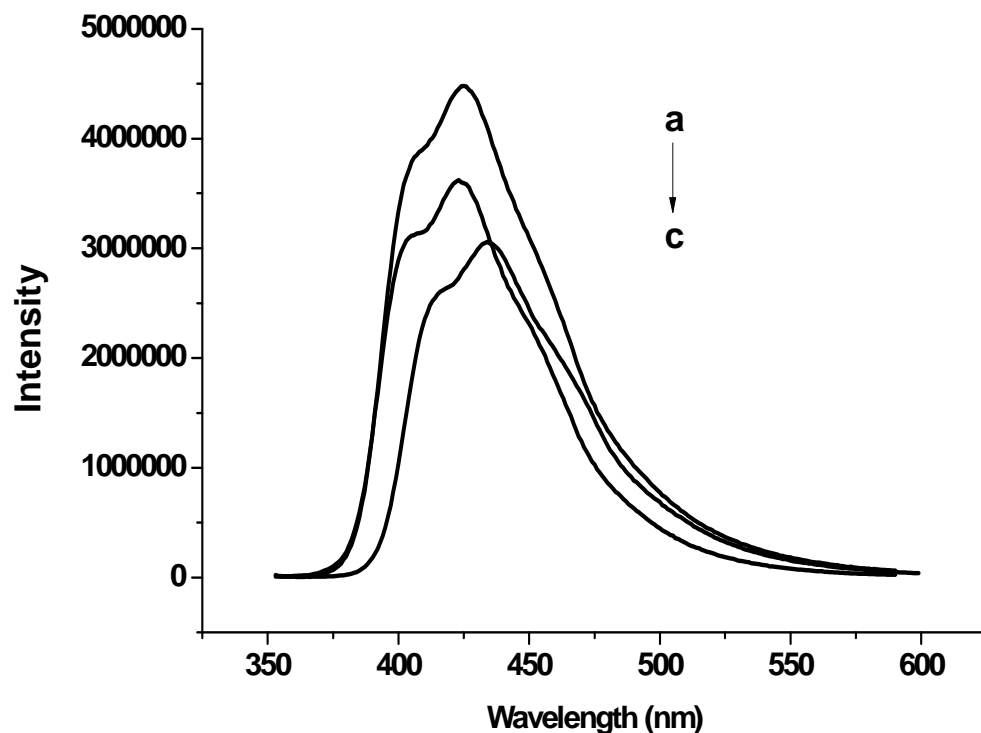


Figure 20. Fluorescence spectra recorded for monomer **M2** (a – c; in THF, dioxane, and chloroform. Concentration of **M2** was 6.32×10^{-6} M and excitation wavelength 350 nm for THF and dioxane and 348 nm for chloroform.

Generally, the emission spectra of **M1** and **M2** in chloroform were red shifted comparing to other solvents considered. This is possibly due to relatively more polar chloroform (Appendix 6) has strong interaction with the fluorophore of the monomers than THF and dioxane. This has the effect of reducing the energy separation between the ground and excited states of monomers in chloroform, which results in a red shift (to longer wavelengths) of the fluorescence emission [36].

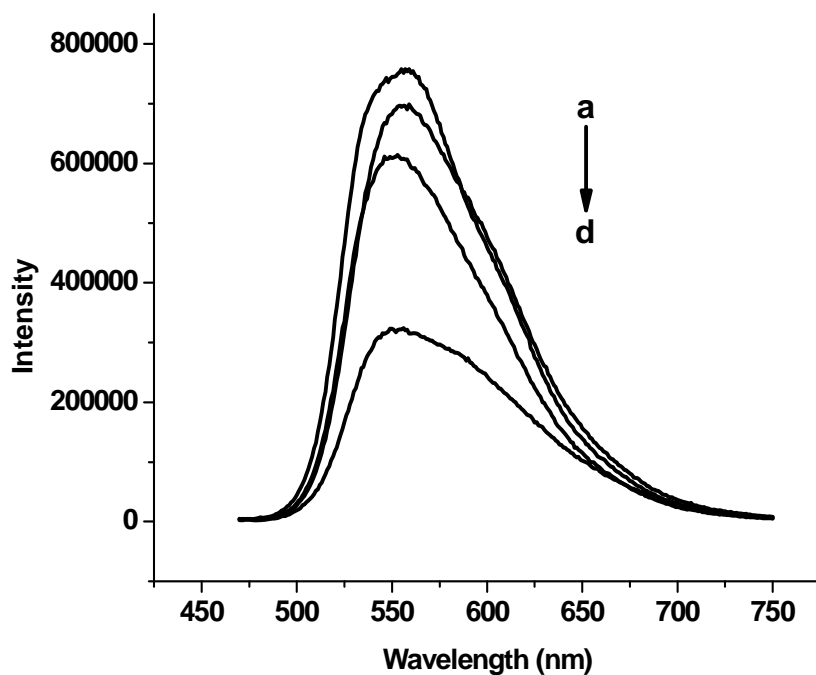


Figure 21. Fluorescence spectra recorded for polymer **P1** (a – d; in toluene, chloroform, THF, and dioxane). Concentration of **P1** was $2.3 \times 10^{-7} \text{M}$ and excitation wavelength 458 nm.

The result in Figure 21 indicates that the emission maximum of **P1** in chloroform, dioxane, toluene, and THF were observed at 559 nm, 556 nm, 555 nm, and 554 nm, respectively. The emission maximum of **P1** in solvents under the study was not significantly changed but the emission intensity was solvent dependent. **P1** in less polar toluene has relatively highest emission intensity than other solvents under study.

Table 2. Absorption (absor.) and emission data for **M1** and **M2**.

Monomers	THF solution		Dioxane solution		Chloroform solution	
	λ max, absor. (nm)	λ max, emission (nm)	λ max, absor. (nm)	λ max, emission (nm)	λ max, absor. (nm)	λ max, emission (nm)
M1	350	420	350	418	348	433, 476
M2	350	425	350	423	348	434

Table 3. Absorption and emission data for polymer **P1**.

P1				
	In chloroform	In THF	In toluene	In dioxane
λ max, absorption (nm)	458	458	458	458
λ max, emission (nm)	559	554	555	556

4.2. Fluorescence ion sensing properties of **M1** and **M2** in different solvents.

In order to study metal ion sensing properties of monomers in different solvents the effect of several metal ions on the fluorescence spectra properties of **M1** and **M2** in THF, chloroform, and dioxane were studied. This was performed by recording fluorescence emission spectra of the materials considered upon addition of different metal ions dissolved in methanol. Results obtained from optical studies confirm that the emission spectra properties (maximum emission wavelength and emission spectra shape) of monomers in THF and dioxane were similar. However, the emission shape and maximum emission wavelength of monomers in chloroform,

especially for **M1** in chloroform was different. Thus, metal ion sensing properties of monomers in chloroform was studied separately from THF and dioxane solutions.

4.2.1. Metal ion sensing properties of **M1** and **M2** in THF and dioxane

The emission spectra of **M1** (6.62×10^{-6} M) and **M2** (6.32×10^{-6} M) in THF after addition of different metal cations are shown in Figure 22 and 23, respectively. Upon addition of 1.0×10^{-2} M each of metal ions in methanol (Na^+ , K^+ , Ca^{2+} , Mg^{2+} , Al^{3+} , Cr^{3+} , Co^{2+} , Ni^{2+} , Cu^{2+} , Cd^{2+} , Zn^{2+} , Hg^{2+} , and Ag^+), no significant change on the fluorescence spectra of **M1** and **M2** were observed. However, the emission intensity of monomers decreased significantly after addition of 1.0×10^{-2} M Fe^{3+} ion in methanol.

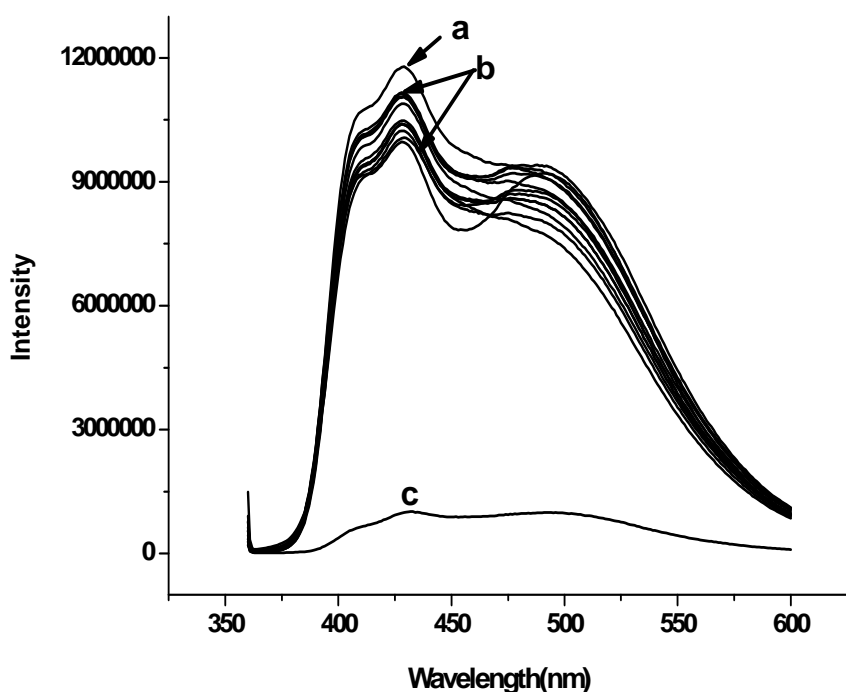


Figure 22. Fluorescence spectra recorded for **M1** (6.62×10^{-6} M) in THF upon exposure to 1.0×10^{-2} M different metal ions in methanol (a. metal free **M1**, b. all metals considered except Fe^{3+} , and c. Fe^{3+}). Excitation wavelength 350 nm.

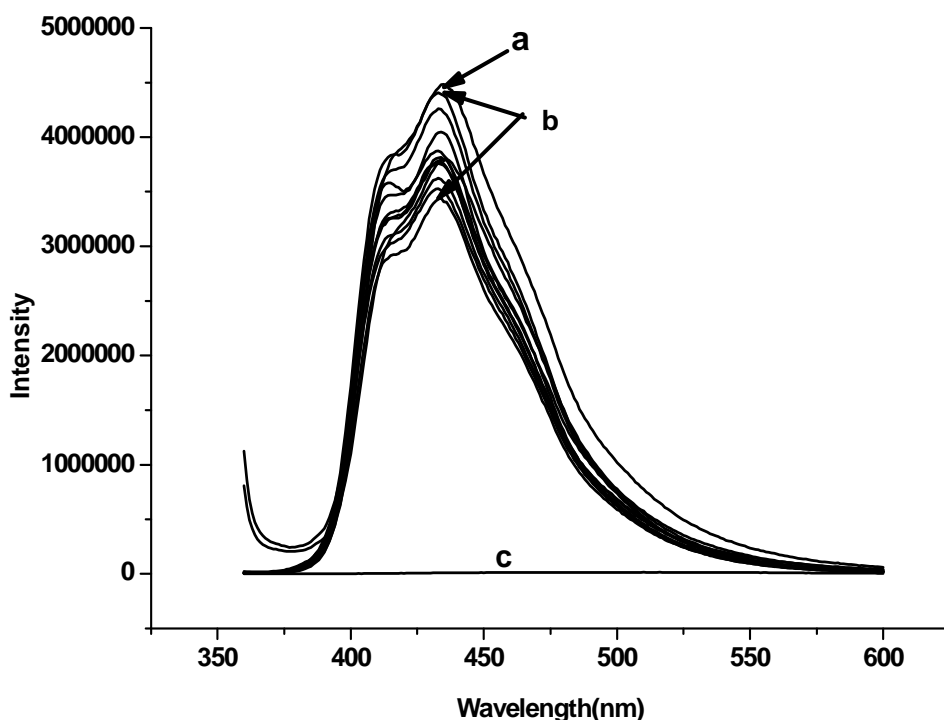


Figure 23. Fluorescence spectra recorded for **M2** (6.32×10^{-6} M) in THF upon exposure to 1.0×10^{-2} M different metal ions in methanol (a. metal free **M2**, b. all metals considered except Fe^{3+} , and c. Fe^{3+}). Excitation wavelength 350 nm.

Similarly, the effects of metal ions on the emission spectra of **M1** and **M2** in dioxane are shown in Appendix 2 and Appendix 3, respectively. Like in THF it is noticeable that the fluorescence intensity, shape and emission maximum of the monomers in dioxane had not significantly changed upon addition of metal ions under the study except for Fe^{3+} ion.

4.2.2. Metal ion sensing properties of M1 and M2 in chloroform

The effect of several metal ions on the fluorescence spectra of **M1** and **M2** in chloroform are shown in Figure 24 and 25, respectively. Like monomers in THF and dioxane the fluorescence spectra properties of **M1** and **M2** were not changed significantly upon addition of the same concentration of metal ions considered in study. However, emission intensity of monomers decreased significantly after addition of 1.0×10^{-2} M Fe^{3+} in methanol.

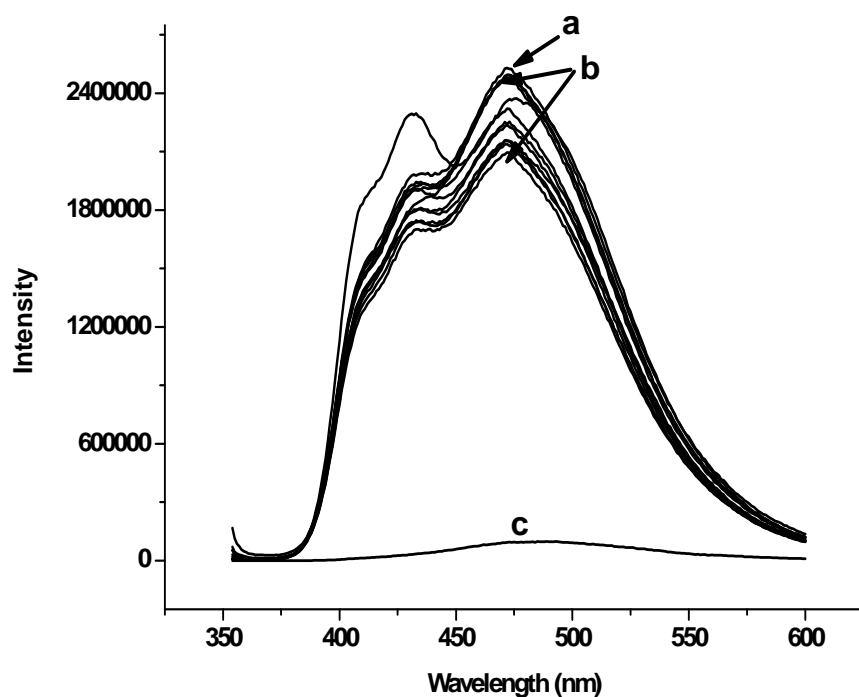


Figure 24. Fluorescence spectra recorded for **M1** (6.62×10^{-6} M) in chloroform upon exposure to 1.0×10^{-2} M different metal ions in methanol (a. metal free **M1**, b. all metals considered except Fe^{3+} , and c. Fe^{3+}). Excitation wavelength 348 nm.

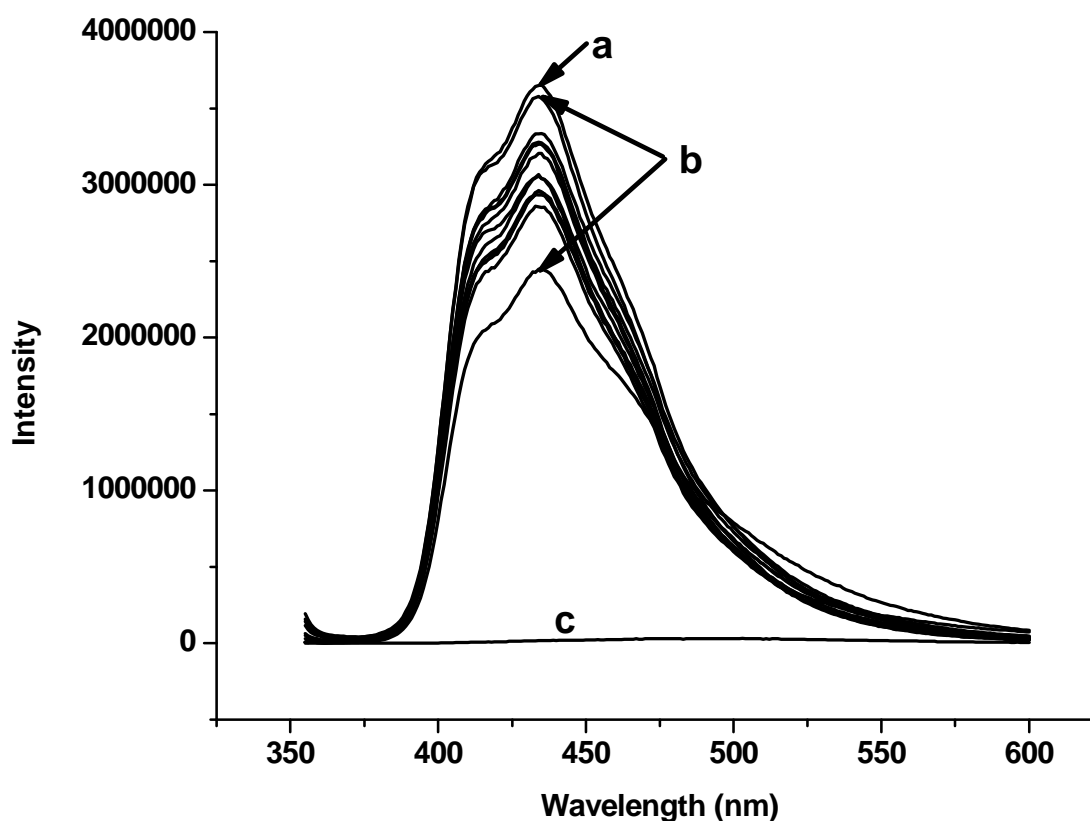


Figure 25. Fluorescence spectra recorded for **M2** (6.32×10^{-6} M) in chloroform upon exposure to 1.0×10^{-2} M different metal ions in methanol (a. metal free **M2**, b. all metals considered except Fe^{3+} , and c. Fe^{3+}). Excitation wavelength 348 nm.

Change in emission intensity of monomers **M1** and **M2** in solvents considered after addition of Fe^{3+} ion is due to the formation of stable complex between the electron deficient trivalent ferric cation and the lone pair electron of nitrogen in imidazole group of monomers. The binding

capacity of the ligands (monomers) to the metal ions is dependent on the cavity size of the ligand and the diameter of the cations. The diameter of Fe^{3+} ion is 1.34 \AA which may fit with the size of the ionophores of the monomers and forms stable complex with it [41].

As it is revealed from optical and metal ion sensing property studies above the response of monomers in THF and dioxane were the same, but chloroform solutions showed different response. Moreover, the emission intensity of monomers in THF was higher than in dioxane. Thus, only monomers in THF and chloroform were selected to study fluorescence response profiles, Stern - Volmer analysis and detection limits.

4.2.3. Relative sensitivity and selectivity of monomers towards metal ions

The possibility of sensing and selectivity of monomer materials towards variety of metal ions are demonstrated based on the fluorescence response profile of **M1** and **M2**. This was investigated from the plot of relative emission intensity ($\frac{I_o}{I}$) versus metal ions, where I_o is emission intensity of metal free monomers and I emission intensity after addition of metal ions. Figure 26 and 27 shows the fluorescence response profile graphs of **M1** and **M2** in THF, respectively. As shown in the fluorescence response profile graphs both monomers showed identical selectivity towards Fe^{3+} ion.

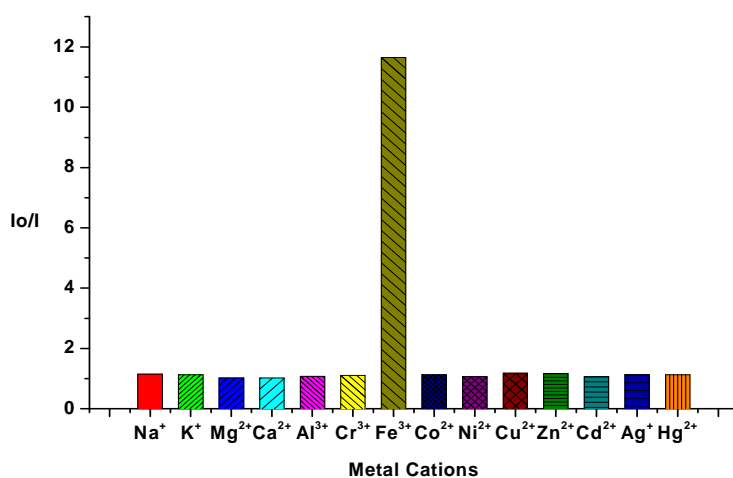


Figure 26. Fluorescence emission response profiles recorded for **M1** (6.62×10^{-6} M) in THF upon exposure to different metal ions (1.0×10^{-2} M) in methanol.

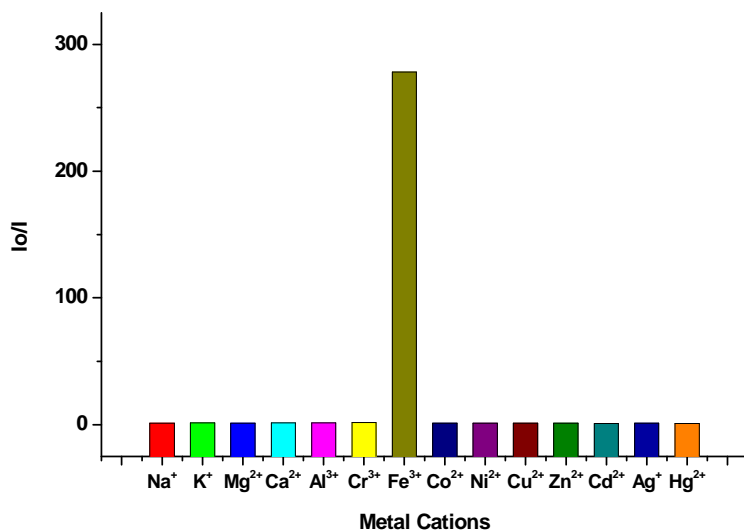


Figure 27. Fluorescence emission response profiles recorded for **M2** (6.32×10^{-6} M) in THF upon exposure to different metal ions (1.0×10^{-2} M) in methanol.

Similarly, the fluorescence response profiles of monomers in chloroform are exhibited in Figure 28 and 29. The results obtained confirm that both monomers showed selectivity to ferric ion only.

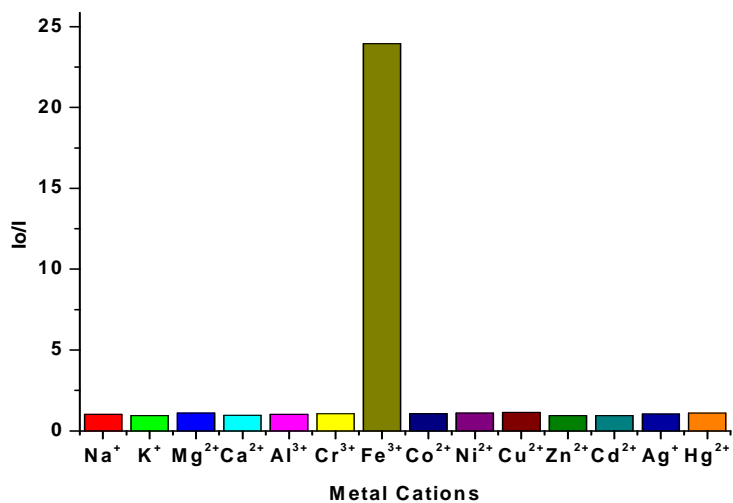


Figure 28. Fluorescence emission response profiles recorded for **M1** in chloroform (6.62×10^{-6} M) upon exposure to different metal ions (1.0×10^{-2} M) in methanol.

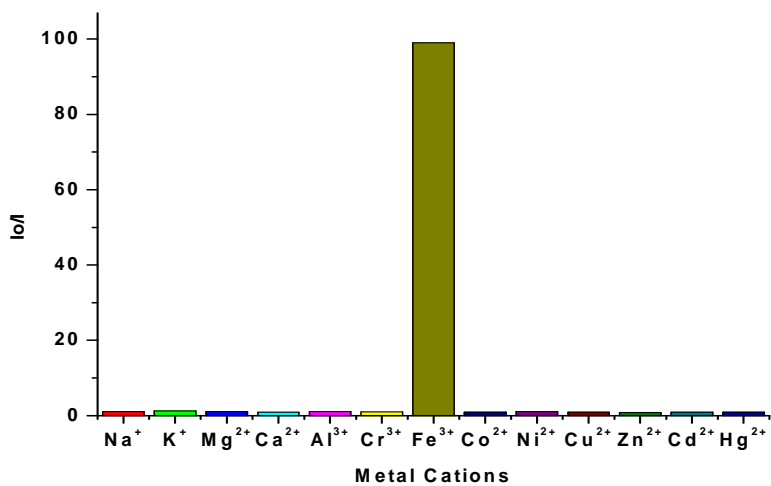


Figure 29. Fluorescence emission response profiles recorded for **M2** in chloroform (6.32×10^{-6} M) upon exposure to different metal ions (1.0×10^{-2} M) in methanol.

Results obtained from the fluorescence profile graphs confirm that monomers **M1** and **M2** were highly sensitive and selective chemosensor materials for Fe^{3+} ion. As shown in fluorescence response profile graphs, with the same experimental conditions, monomer **M2** is more sensitive to Fe^{3+} ion than **M1**. In addition, Fe^{3+} ion have been relatively more efficiently to quench the fluorescence intensity of the monomers in THF than in chloroform.

4.2.4. Stern-Volmer analysis for response of monomers in THF and chloroform to Fe^{3+} ion.

The fluorescence emission intensity change of monomers **M1** and **M2** in THF upon addition of different concentrations of ferric ion are exhibited in Figure 30 and 31, respectively. The results showed that the emission intensity was linearly changed with increasing ferric ion concentration. So for **M1** and **M2** in THF, the Fe^{3+} ion responsive property was based on decreasing of fluorescence intensity (fluorescence quenching).

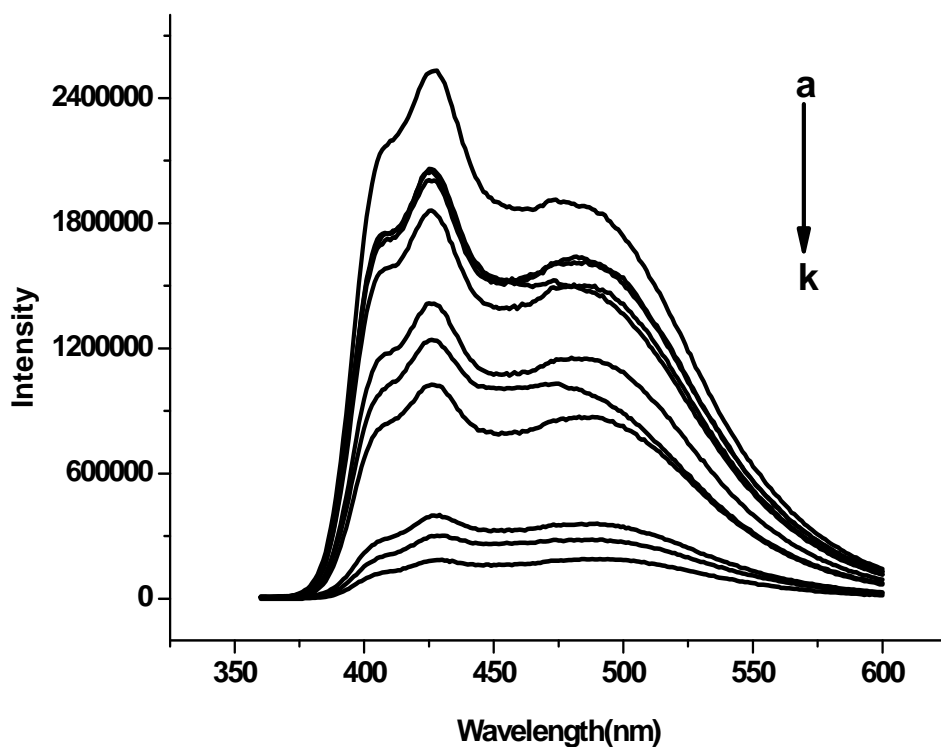


Figure 30. Fluorescence spectra recorded for **M1** (6.62×10^{-6} M) in THF upon exposure to different concentrations of ferric ion (a - k; ferric ion free **M1**, 1.0×10^{-6} , 8.0×10^{-6} , 1.0×10^{-5} , 6.0×10^{-5} , 2.0×10^{-4} , 8.0×10^{-4} , 1.0×10^{-3} , 4.0×10^{-3} , 6.0×10^{-3} , and 8.0×10^{-3} M in methanol). Excitation wavelength 350 nm.

Emission intensity quenching at various concentrations of ferric ion have been used to compare the sensing ability of **M1** and **M2** towards Fe^{3+} ion based on Stern - Volmer analysis. Stern - Volmer equation ($\frac{I_0}{I} = 1 + K_{sv}[Q]$), where I_0 intensity of the monomers without ferric cation, I intensity of monomers after addition of various concentration of ferric cation, K_{sv} is Stern - Volmer constant and $[Q]$ is concentration of the quencher that is ferric ion used to compare the sensitivity of the monomers quantitatively [9].

According to Stern-Volmer equation, when all other variables are held constant, the higher the K_{sv} , the lower the concentration of ferric required to quench the emission intensity. The value of K_{sv} is easily determined from the slope of the plot intensity change versus concentration of Fe^{3+} ion [9].

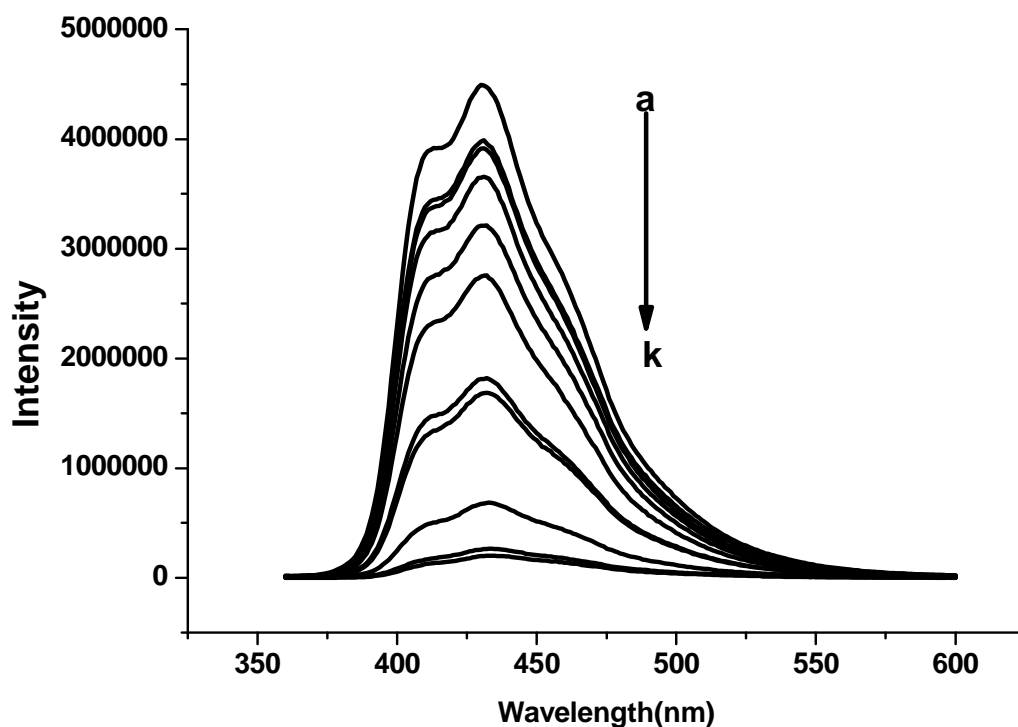


Figure 31. Fluorescence spectra recorded for **M2** (6.32×10^{-6} M) in THF upon exposure to different concentrations of ferric ion (a - k; ferric ion free **M2**, 1.0×10^{-6} , 8.0×10^{-6} , 1.0×10^{-5} , 6.0×10^{-5} , 2.0×10^{-4} , 8.0×10^{-4} , 1.0×10^{-3} , 4.0×10^{-3} , 6.0×10^{-3} , and 8.0×10^{-3} M in methanol). Excitation wavelength 350 nm.

The Stern-Volmer plots for monomers in THF are shown in Figure 32 and 33, respectively. The values of Stern -Volmer constant (K_{sv}) for **M1** and **M2** in THF calculated from the slope of the plots were $6.474 \times 10^2 \text{ M}^{-1}$ and $1.495 \times 10^3 \text{ M}^{-1}$, correspondingly.

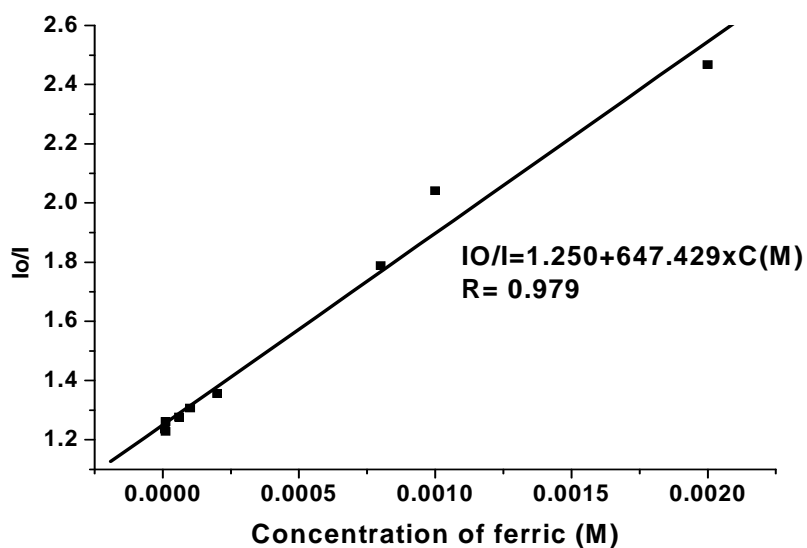


Figure 32. Stern - Volmer plot for emission intensity quenching of **M1** in THF at various concentrations of Fe^{3+} ion.

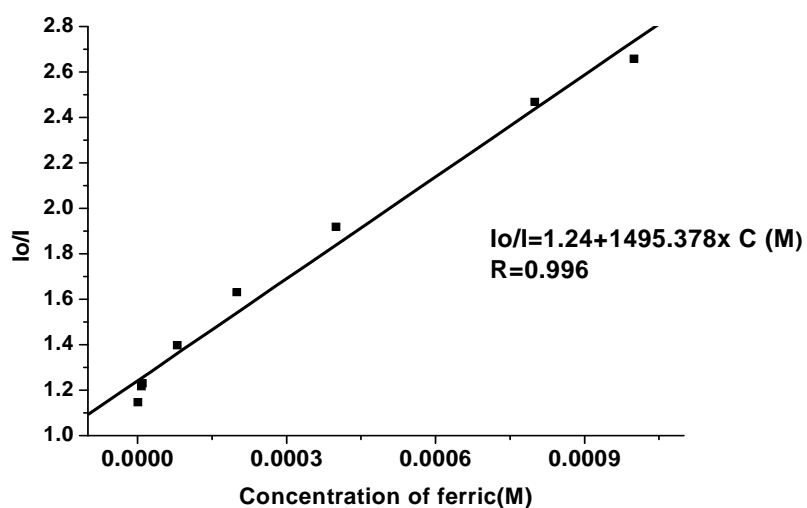


Figure 33. Stern - Volmer plot for emission intensity quenching of **M2** in THF at various concentrations of Fe^{3+} ion.

Similarly, the fluorescence emission intensity change of monomers **M2** and **M1** in chloroform upon addition of different concentrations of ferric ion are exhibited in Figure 34 and 35, respectively. As in the case of THF solution, the emission intensity was quenched linearly with increasing the concentration of ferric ion for both monomers. However, upon coordination with ferric ion the lower emission peak formed at 433 nm for **M1** in chloroform was disappeared. Hence, for **M1** in chloroform the longer emission peak at 476 nm was used for Stern - Volmer analysis.

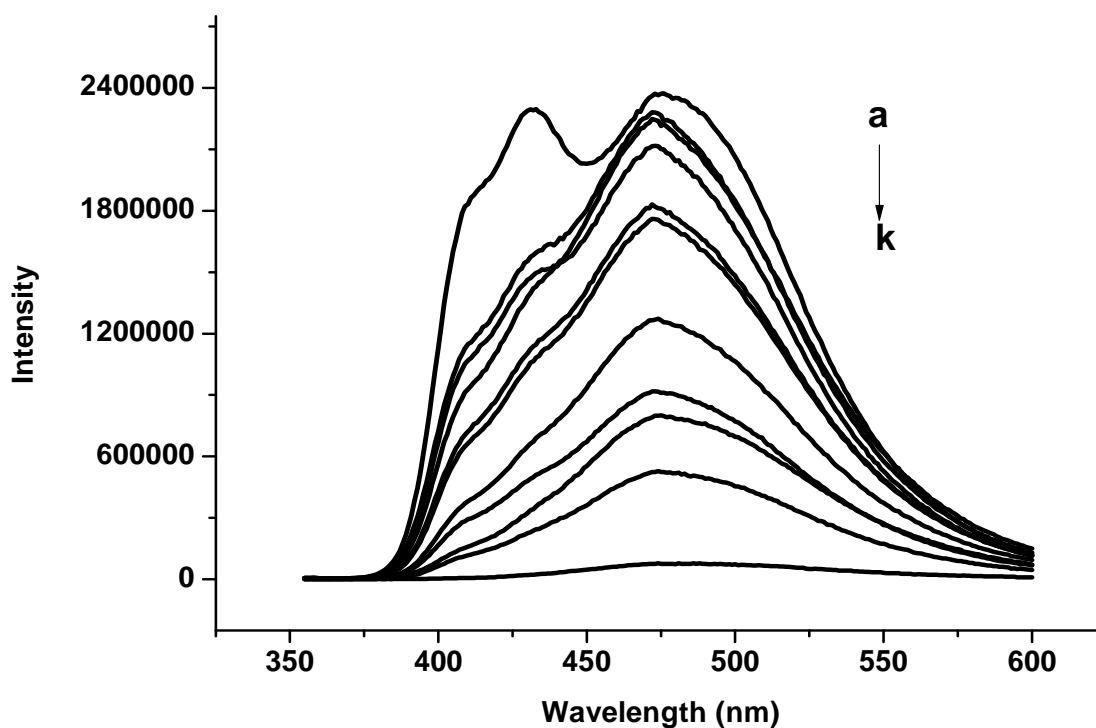


Figure 34. Fluorescence spectra recorded for **M1** (6.62×10^{-6} M) in chloroform upon exposure to different concentrations of ferric ion (a - k; ferric ion free **M1**, 1.0×10^{-6} , 8.0×10^{-6} , 1.0×10^{-5} , 6.0×10^{-5} , 2.0×10^{-4} , 8.0×10^{-4} , 1.0×10^{-3} , 4.0×10^{-3} , 6.0×10^{-3} , and 8.0×10^{-3} M in methanol). Excitation wavelength 350 nm.

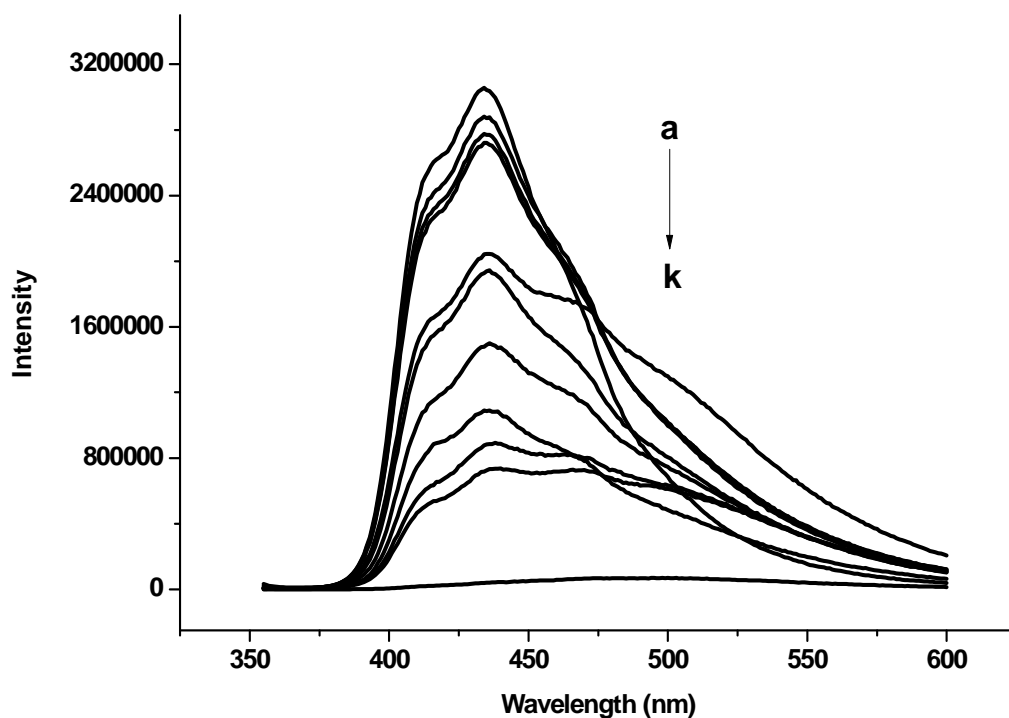


Figure 35. Fluorescence spectra recorded for **M2** (6.32×10^{-6} M) in chloroform upon exposure to different concentrations of ferric ion (a - k; ferric ion free **M2**, 1.0×10^{-6} , 8.0×10^{-6} , 1.0×10^{-5} , 6.0×10^{-5} , 2.0×10^{-4} , 8.0×10^{-4} , 1.0×10^{-3} , 4.0×10^{-3} , 6.0×10^{-3} , and 8.0×10^{-3} M in methanol). Excitation wavelength 350 nm.

The Stern - Volmer plots for **M1** and **M2** in chloroform at all concentration of Fe^{3+} ions are shown in Figure 36 and 37, correspondingly. The value of Stern - Volmer constant (K_{sv}) obtained from the slope of the plots for the interaction between Fe^{3+} ion and the monomers in chloroform were $3.928 \times 10^2 \text{ M}^{-1}$ and $5.535 \times 10^2 \text{ M}^{-1}$, respectively.

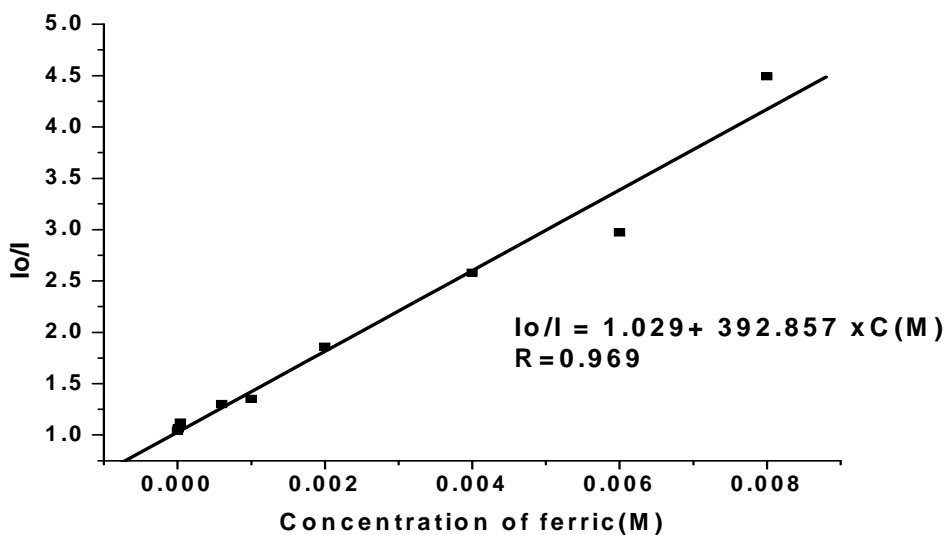


Figure 36. Stern - Volmer plot for emission intensity quenching of **M1** in chloroform at various concentrations of Fe^{3+} ion.

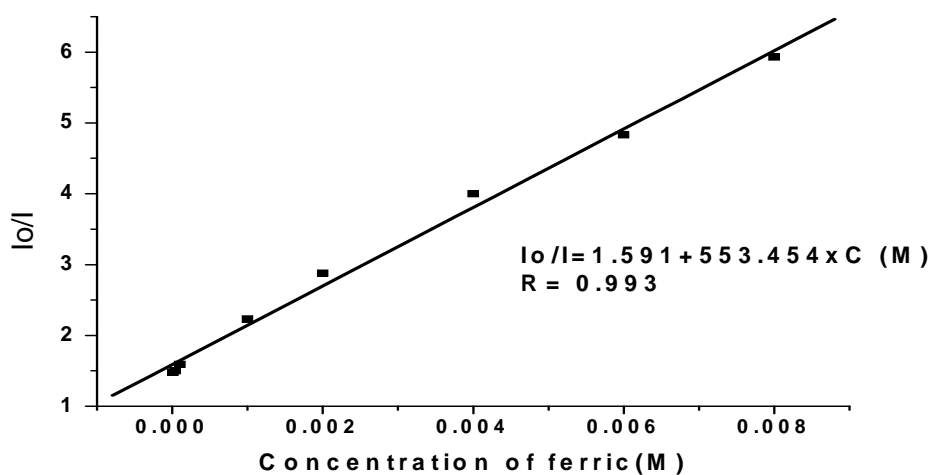


Figure 37. Stern - Volmer plot for emission intensity quenching of **M2** in chloroform at various concentrations of Fe^{3+} ion.

When the nature of the Stern - Volmer plots is examined in all solvents under study it shows linear dependence of $\frac{I_0}{I}$ on Fe^{3+} ion concentration, with corresponding regression coefficients (R) value summarized in Table 4. Which indicates the formation of none fluorescence ground state complex between the monomers and the quencher i.e., Fe^{3+} . The mechanism of quenching and the type of quenching in this case of formation of stable complex between the ionophore and the cation is photoinduced electron transfer (PET) and static quenching, respectively [9].

Table 4. Stern-Volmer constant values for **M1** and **M2**.

	M1		M2	
	In THF	In chloroform	In THF	In chloroform
K _{sv} (M ⁻¹)	6.474x10 ²	3.928x10 ²	1.49510 ³	5.535x10 ²
Regression Coefficient(R)	0.979	0.996	0.969	0.993

Large value of K_{sv} in Stern - Volmer analysis indicates the efficiency of quenching. So according to results found ferric cation was relatively more effective to quench the intensity of **M2** than **M1** in THF and chloroform. However, monomers dissolved in THF were more sensitive to ferric ion. High sensing ability of **M2** compared with **M1** may be due to the presence of electron donating methoxy group in the monomer backbone which may increase electron density on the **M2** backbone [35].

4.2.5. Detection limit for quantitative analysis of ferric cation.

The point at which the analyte becomes feasible or limit of detection (LOD) for monomers **M1** and **M2** were calculated based on statistical approach. In this approach a series of blank (samples that do not contain analyte) were tested and the mean blank value and standard deviation were calculated [48]. To calculate LOD first we measured replicated fluorescence intensity (10

measurements) for metal free monomers in methanol solvent and from these values standard deviation-n of the blank was calculated. The numerical value of limit of detection is calculated using $\frac{3Sd}{m}$ [48], where Sd is standard deviations of the blank and m is slope the calibration curve. The calibration curves for monomers in THF are shown in Figure 38 and 39, respectively. The slopes calculated for **M1** and **M2** in THF were 2.550×10^{-4} and 3.335×10^{-4} , respectively.

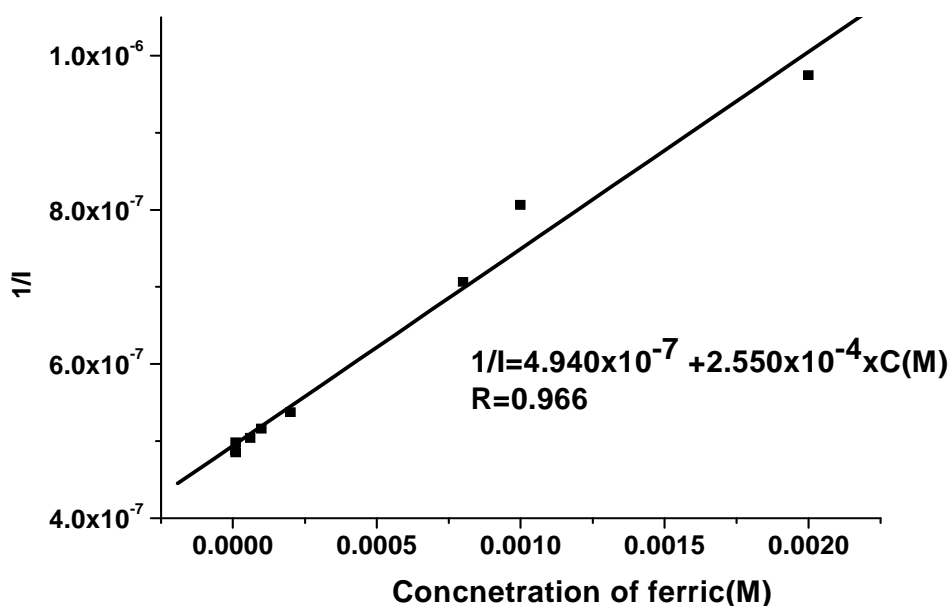


Figure 38. Calibration curve for monomer **M1** in THF at various concentrations of ferric ion.

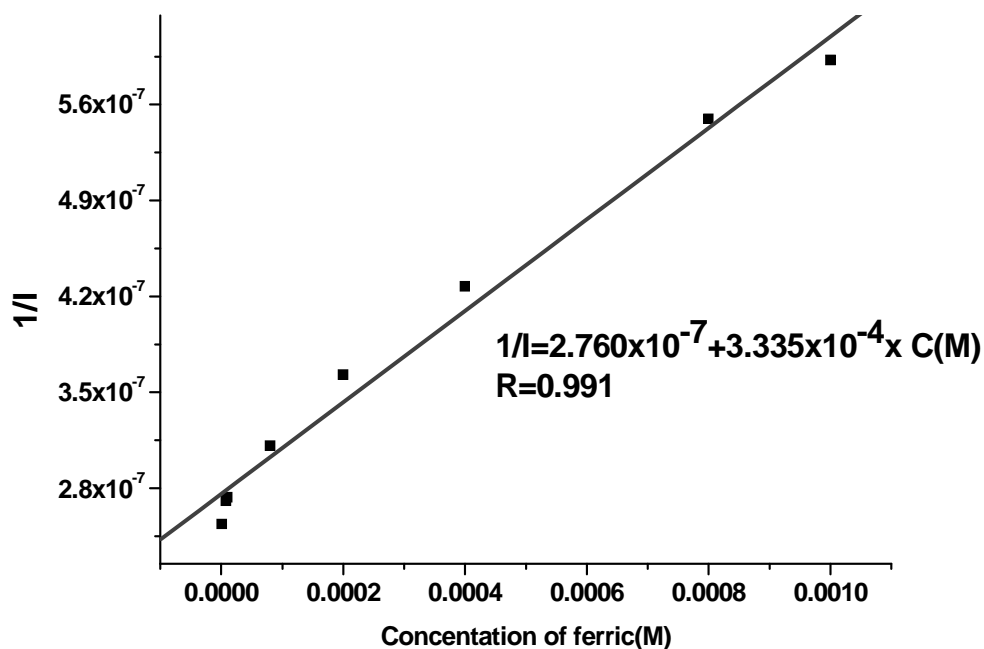


Figure 39. Calibration curve for monomer **M2** in THF at various concentrations of ferric ion.

Finally, from the slope and the standard deviation of the blanks the limit of detection was calculated mathematically and the LOD values for **M1** and **M2** were 1.386×10^{-5} M and 3.902×10^{-6} M, correspondingly.

Similarly, the calibration curves for both monomers in chloroform upon addition of different concentrations of ferric ion are shown in Figure 40 and 41, respectively. The detection limits obtained for **M1** and **M2** in chloroform were 1.315×10^{-5} M and 3.707×10^{-5} M, correspondingly.

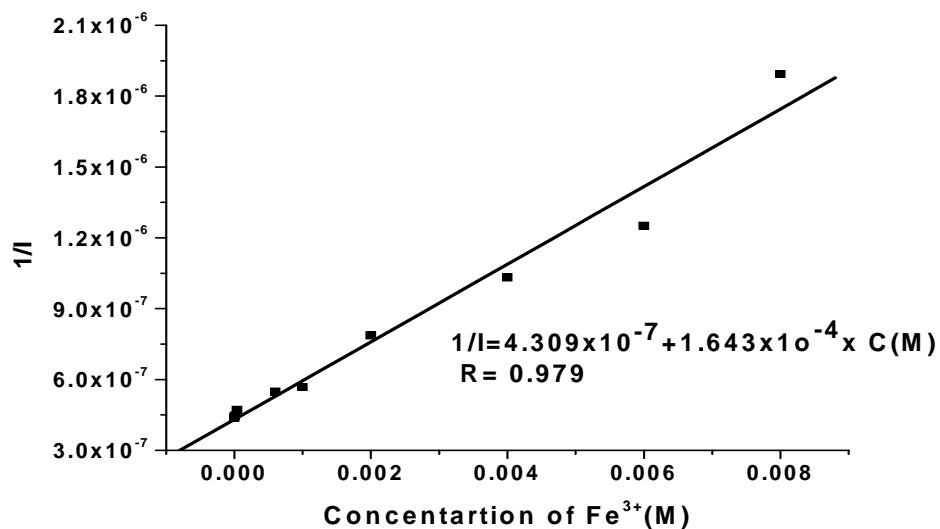


Figure 40. Calibration curve for monomer **M1** in chloroform at various concentrations of ferric ion.

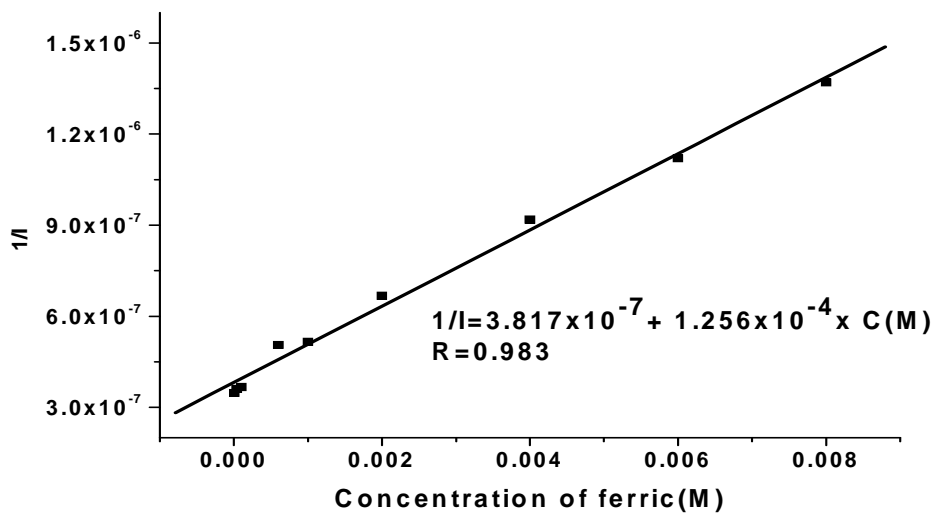


Figure 41. Calibration curve for monomer **M2** in chloroform at various concentrations of ferric ion.

Calculated value of the limit of detection (LOD) for **M1** and **M2** in THF and chloroform upon addition of various concentrations of ferric ions are summarized in table 5. The results obtained showed that **M2** has relatively better sensing ability for ferric ion than **M1**.

Table 5. Limit of detection values for **M1** and **M2**.

	M1		M2	
	In THF	In chloroform	In THF	In chloroform
Standard deviation	1.180×10^{-9}	7.208×10^{-10}	4.338×10^{-10}	1.553×10^{-9}
Slope	2.550×10^{-4}	1.643×10^{-4}	3.335×10^{-4}	1.256×10^{-4}
LOD (mol L ⁻¹)	1.386×10^{-5}	1.315×10^{-5}	3.902×10^{-6}	3.707×10^{-5}

4.3. Fluorescence cation sensing properties of **P1** in different solvents.

Solvents may cause change in the intensity, position and shape of emission band of conducting polymers [48]. Herein, the ion sensing properties of **P1** was investigated in different solvents.

Figure 42 presents the fluorescence spectra of **P1** in toluene during addition of different metal ions. Upon addition of each 1.0×10^{-2} M metal ions in methanol (Na⁺, K⁺, Mg²⁺, Ca²⁺, Al³⁺, Cr³⁺, Co²⁺, Ni²⁺, Cu²⁺, Zn²⁺, Cd²⁺, Ag⁺, and Hg²⁺) no obvious changes of emission spectra were observed. Whereas, relatively little fluorescence quenching was observed in presence of Fe³⁺.

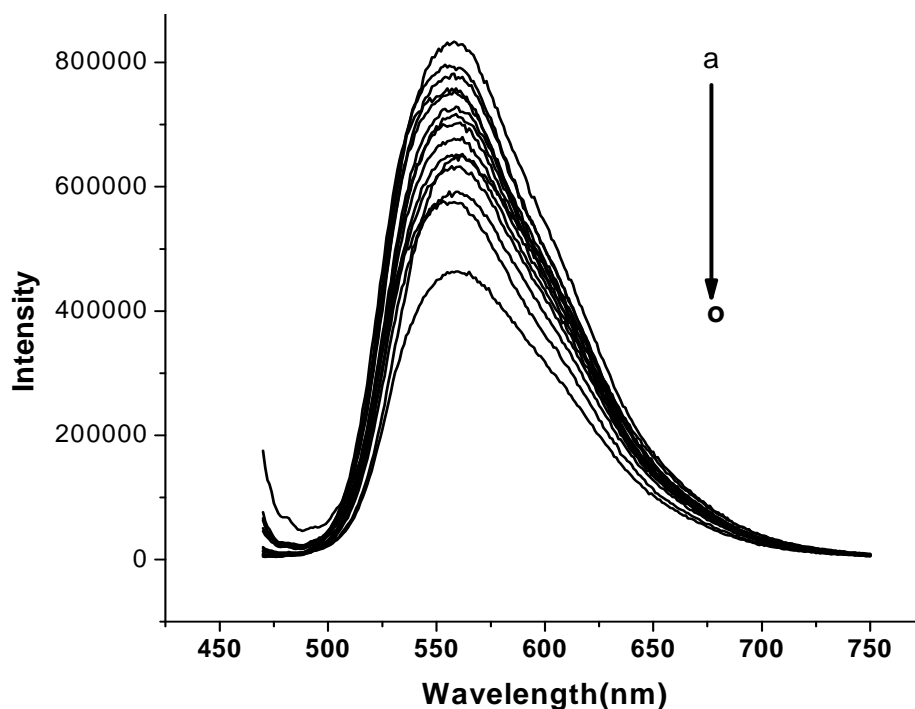


Figure 42. Fluorescence spectra recorded for **P1** (2.3×10^{-7} M) in toluene upon exposure to different metal cations (1.0×10^{-2} M) in methanol (a - o; metal free **P1**, Ag^+ , Co^{2+} , Mg^{2+} , K^+ , Ni^{2+} , Hg^+ , Cu^{2+} , Cd^{2+} , Na^+ , Ca^{2+} , Zn^{2+} , Cr^{3+} , Al^{3+} , and Fe^{3+}). Excitation wavelength 458 nm.

The fluorescence response profile of the polymer **P1** in toluene upon addition of different metal cations are investigated, as shown in Figure 43. Almost all metal ions did not any effect on the emission spectra of **P1** in toluene, while Fe^{3+} had little quenching effect on the fluorescence spectra of **P1**. This is due to there was no stable complex between the binding site of **P1** and the metal ions selected. So **P1** dissolved in toluene could not be selective and sensitive chemosensor for metal ions included in the study.

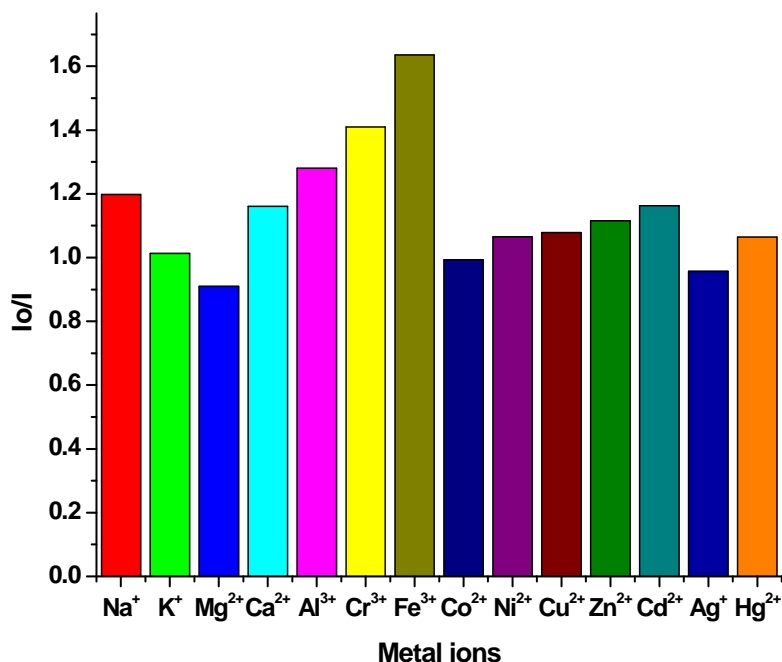


Figure 43. Fluorescence response profile of **P1** (2.3×10^{-7} M) in toluene upon addition of different metal ions (1.0×10^{-2} M) in methanol.

To demonstrate the effect of solvents on the sensing ability of **P1** the emission spectra in chloroform, THF and dioxane upon addition of metal ions was studied. As shown in Figure 44, Appendix 4 and Appendix 5 metal ions considered had negligible effects on the fluorescence spectra properties of the polymer **P1** in chloroform, THF and dioxane, respectively.

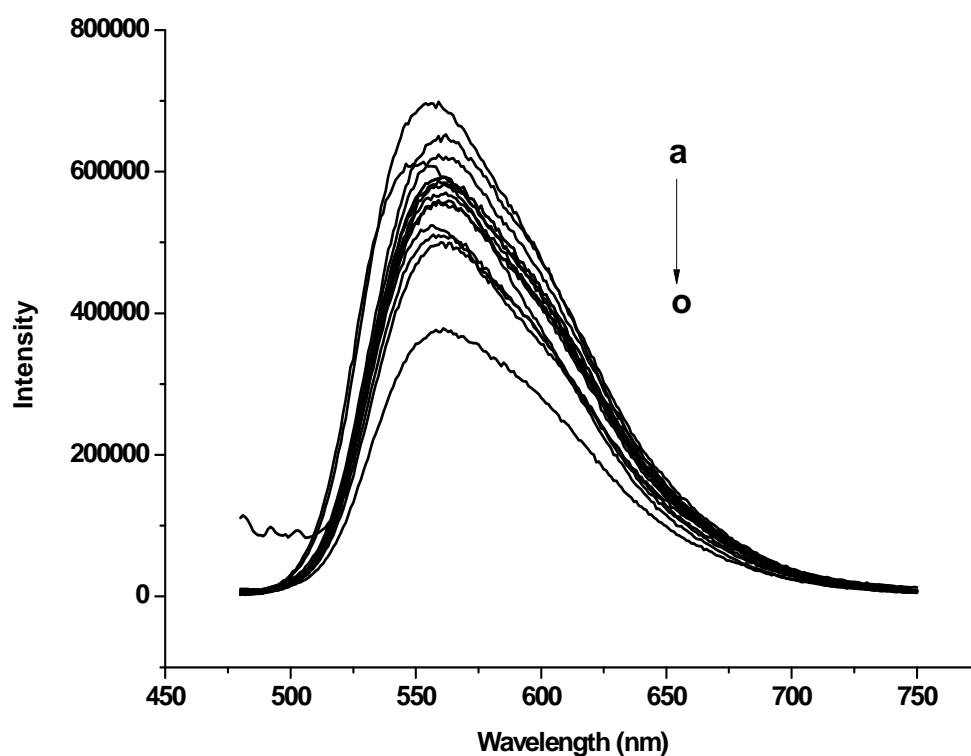


Figure 44. Fluorescence spectra recorded for **P1** (2.3×10^{-7} M) in chloroform upon exposure to 1.0×10^{-2} M of different cations in methanol (a - o; metal free **P1**, K^+ , Ca^{2+} , Na^+ , Zn^{2+} , Cd^{2+} , Mg^{2+} , Co^{2+} , Ag^+ , Ni^{2+} , Hg^+ , Cr^{3+} , Cu^{2+} , Al^{3+} , and Fe^{3+})

Results obtained confirm that conjugated polymer **P1** in solvents considered cannot form any stable complex with the metal ions included in the study and it would not be used as active site in chemosensory systems to sense metal ions. This is possibly due to the metal size may not fit the coordination ability of thiazole or thiophene ligand in the backbone to form stable complex or the long pentyl chains in the polymer backbone may affect the interaction between the quenchers (metal ions) and the recognition units in the polymer [47].

5. Conclusions

Imidazole containing monomers (**M1** and **M2**) and conjugated polymer **P1** which contain thiophenes and thiazoles in the polymer backbone have been used for metal ion chemosensor studies using fluorescence spectroscopy. The optical properties and metalloreactivity of monomers **M1** and **M2** showed almost similar response in chloroform, THF, and dioxane. Structurally rigid conjugated polymer (**P1**) in chloroform, toluene, THF, and dioxane not showed any significant change in its fluorescence emission properties upon addition of different metal ions.

The fluorescence intensities changed linearly according to the concentration of ferric ion for both monomers in solvents under the study, indicating that these monomeric materials would be an effective sensing material for ferric ion. The Stern - Volmer constant value of **M2** is 23 times higher than **M1** both in THF, which confirms that Fe^{3+} ion have been relatively more efficiently to quench the fluorescence intensity of monomer **M2** than monomer **M1**. In contrast, the emission spectra of conjugated polymer **P1** was insensitive to all metal ions considered.

Finally, results obtained showed that the monomers containing imidazole group would be used as active materials for application in fluorescence chemosensor for Fe^{3+} ion and their sensitivity and selectivity were not affected by solvent polarity considered in the study.

6. References

1. Gao, T.; Lee, M. K.; Hoe, J.; Yang, S. *A New Ferric Ion - Selective Fluorescence Chemosens -or with Wide Dynamic Range*, Bull. Korean Chem. Soc., **2010**, 31, 2100 - 2102.
2. Zhang, Y.-M.; Chen, Y.; Li, Z.-Q.; Li, N; Liu, Y. *Quinolinotriazole - β - cyclodextrin and Its Adamantanecarboxylic Acid Complex as Efficient Water-Soluble Fluorescent Cd^{2+} Sensors*, Bioorg. Med. Chem., **2010**, 18, 1415 – 1420.
3. Quang, D.T.; Kim, J.S. *Fluoro- and Chromogenic Chemodosimeters for Heavy Metal Ion Detection in Solution and Biospecimens*, Chem. Reviews, **2010**, 30, 5 - 22.
4. Dai, L.; Soundarrajan P.; Kim, T. *Sensors and sensor arrays based on conjugated polymers and carbon nanotubes*, Pure Appl. Chem., **2002**, 74, 1753 – 1772.
5. Ripka, P.; Tipek, A. *Hand Book of Modern Sensors*, 1st ed., ISTE LTD: London, **2007**, 49 – 80.
6. Grundler, P. *Chemical sensor: an introduction to scientists and engineers*, 5th ed., Springer: Berlin, **2007**, 1 - 13.
7. Janta, J. *principles of chemical sensors*, 1st ed., plenum: New York, **1989**, 1 - 36
8. Eggins, B.R. *Principles of chemical sensors and Biosensors*, 2nd ed., Willey: New York, **2006**, 1 - 7.
9. Lakowicz, J.R. *Principles of Fluorescence Spectroscopy*, 3rd ed., Springer: Berlin, **2006**, 1 - 351.
10. Skoog, A.D.; Holler. J.F.; West, D.M. *Fundamentals of Analytical Chemistry*, 7th ed., Thomsen learning, **2007**, 601 - 609.
11. Valeur, B. *Molecular Fluorescence: Principles and Applications*, Wiley: Germany, **2001**, 1 - 113.
12. Atkins, P.; Paula, J. D. *Physical Chemistry*. 7th, ed., Oxford: New York, **2002**, 550 - 553.
13. Harris, D.C. *Quantitative Chemical Analysis*, 4th ed., W.H Freeman and Company: New Work, **1995**, 536 - 546.
14. Schulman, S.G. *Fluorescence and Phosphorescence Spectroscopy: Physicochemical Principle and Practice*, Pergamon, **1979**, 1 - 65.

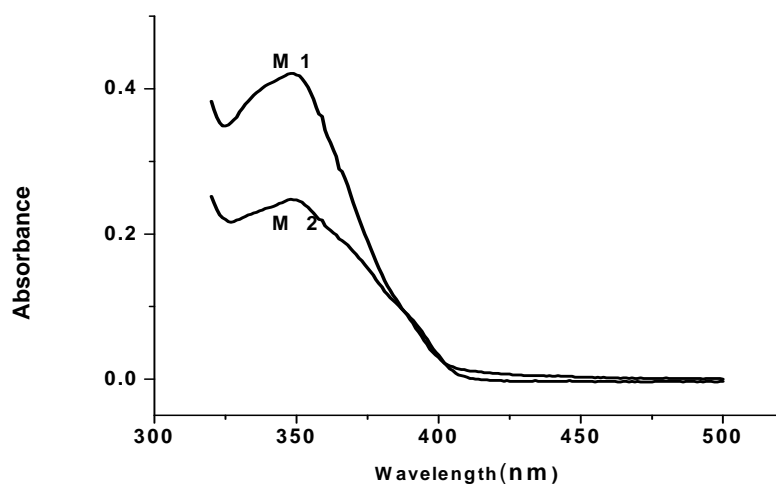
15. Fan, L.;Zhang, Y.;Murphy, C.B;Angell, S.E;Parker; M.F.L;Flynn, B.R.; Jones Jr. *Fluorescence Conjugated Polymer Molecular Wire Chemosensors for Transition Metal Ion Recognition and Signaling*, Coord. Chem. review, **2009**, 253,410 - 422.
16. Retting, W. Strehmel, B.; Schrader, B.; Seifer, H. *Applied Florescence in Chemistry, Biology and Medicine*, Springer: Germany, **1999**, 112 - 150.
17. Tong, H.; Wang, L.; Jing, X.; Wang, F. Solvent Effects of a Fluorescence polyquinoline Chemosensor for Metal Ions, *Macromol. Rapid Commun.*, **2002**, 23,877 - 880.
18. Barford, W. *Electronic and Optical Properties of Conjugated Polymers*, 1st ed., Oxford: New York, **2005**, 20 - 64.
19. Chandrasekhar P. *Conducting Polymers, Fundamentals and Application a Practical Approach*, Kluwer Academic Publishers: London, **1999**, 1 - 45.
20. Leray, I; Valeur, B. *Calixarene-Based Fluorescent Molecular Sensors for Toxic Metals*, *Eur. J. Inorg. Chem.*, **2009**.
21. Zhou, Q.; Swager, T. M. *Fluorescent Chemosensors Based on Energy Migration in Conjugated Polymers: The Molecular Wire Approach to Increased Sensitivity*, *J. Am. Chem. Soc.*, **1995**,117, 12593 - 12602.
22. Na J.; Kim, Y.; Park, W.H.; Lee, T.S. *Metal-Induced Optical Sensing and Optical Switching in Poly (pyridyl phenylene)*, *J. Polym. Sci. Part A: Polym. Chem.*, **2004**, 42, 2444–2450.
23. Wolfbeis, O.S. *Materials for Fluorescence-Based Optical Chemical Sensors*, *J. Mater. Chem.*, **2005**, 15, 2657 – 2669.
24. Fan, L.-J.; Zhang Y.; Jones, J.; W.E. *Design and Synthesis of Fluorescence “Turn-on” Chemosensors Based on Photoinduced Electron Transfer in Conjugated Polymers*, *Macromolecules*, **2005**, 38, 2844 - 2849.
25. Wang, B.; Wasielewski, M.R. *Design and Synthesis of Metal ion-recognition-induced Conjugated Polymers: an Approach to Metal Ion Sensory Materials*, *J. Am. Chem. Soc.*, **1997**, 12 - 21.
26. Albinsson, B. *Dual Fluorescence from N⁶,N⁶-Dimethyladenosine*, *J. Am. Chem. Soc.*, **1997**, 119, 6369 - 637.

27. Al-Kady, A.S.; Gaber, M.; Hussein, M.M.; Ebeid, M. *Fluorescence Enhancement of Coumarin Thiourea Derivatives by Hg²⁺, Ag⁺, and Silver nanoparticles*, J. Phys. Chem. **2009**, 113, 9474 – 9484.
28. Nishimura, Y.; Takemura, T.; Araia, S. *Effective Na⁺ Fluorescent Sensing by New Podand-type Receptor Connecting Two Pyrene Units and Diphenyl Ether*, ARKIVOC, **2009**, 43 - 50.
29. Chen, J.; Cao, S.; Wang D.; Wang, X. *A Phenol-based Compartmental Ligand as a Potential Chemosensor for Zinc (ii) Cations*, J. Brazilian Chem. Soc., **2009**, 20, 14 - 20.
30. Kawakami, T.; Hisada, Y.; Shibutani, Y. *A Cu²⁺ Ion-Selective Fluoroionophore with Dual Off/on Switches*, Chemistry Central Journal, **2010**, 2 - 6.
31. Lee, T.S.; Yang, C.; Kim, J.L.; Lee, J.K.; Park, W.H.; Won, W.J. *Synthesis of Polyquinoline Ether and Its Optical Sensor Property in the Presence of Metal Cations*, J. Polym. Sci. Part A: Polym. Chem., **2002**, 40, 1831 – 1837.
32. Qin, C.; Cheng, Y.; Wang, L.; Jing, X.; Wang, F. *Phosphate-functionalized Polyfluorene as a Highly water –Soluble Iron (III) Chemosensor*, Macromolecules, **2008**, 41, 7798 - 7804.
33. Zhou, X-H.; Yan, J.-C.; Pei, J. *Exploiting an Imidazole-Functionalized Polyfluorene Derivatives as a chemosensory Material*, Macromolecules, **2004**, 37, 7078 - 7080.
34. Reichardt, C. *Solvatochromic Dyes as Solvent Polarity Indicators*, Chem. Rev., **1994**, 94, 2319 - 2358.
35. Gao, Y.; Bai, H.; Shi, G. *Electrosynthesis of oligo (methoxy pyrene) for turn-on fluorescence detection*, J. matter. Chem., **2010**, 20, 2993 - 2998.
36. Barghouthi, S.A.; Perrault, J.; Holmes, L.H. *Effect of Solvents on the Fluorescence Emission Spectra of 1-Anilino-8-Naphthalene Sulfonic Acid: A Physical Chemistry Experiment*, Springer-Verlag: New York, **1998**, 3, 1 - 10.
37. Jędrzejewska, B.; Pączkowsk, J, J. *Solvent Effects on the Spectroscopic Properties of Styrylquinolinium Dyes Series*, J. Fluoresc., **2010**, 20, 73 - 86.
38. Lee, J.K.; Lee, T.S. *Newly Synthesized Polybenzoxazole Derivative with an Adjacent Hydroxyphenyl Ring for Optical Sensing*. Polym. Sci. Part A: Polym. Chem., **2005**, 43, 1397 – 1403.

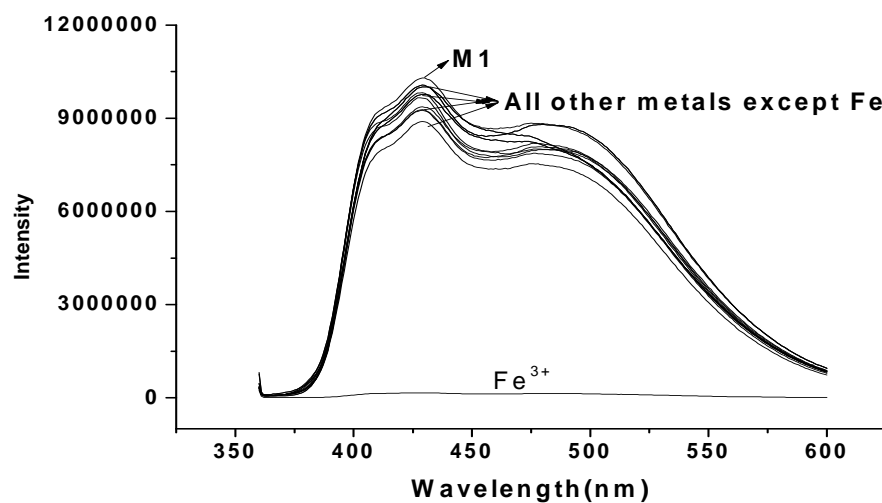
39. Zhou, G. Qian, G. Ma, L.; Cheng, Y.; Xie, Z.; Wang, L.; Jing, X.; Wanfg, F. *Polyfluorenes with Phosphate Group in the Side Chains as Chemosensors and Electroluminescent Materials*, *Macromolecules*, **2005**, 38, 5416 - 5424.
40. Okamoto, H.; Satake, K.; Kimura, M. *Fluorescence Properties of 3- and 4-Trifluoroacetyl-amino-1, 8-Naphthalimides: Solvent-Controlled Switching of Fluorescence Color and Response to Metal-Cations*, *ARKIVOC*, **2007**, 112 - 123.
41. Lakowicz, J.R. *Probe Design and Chemical Sensing*, Plenum Press: New York, **1994**, 21-28.
42. Feng, J.; Li, Y.; Yang, M. *Hyperbranched Copolymer Containing Triphenylamine and Divinyl Bipyridyl Units for Fluorescent Chemosensors*, *J. Polym. Sci. Part A: Polym. Chem.*, **2009**, 47, 222 – 230.
43. Kertesz, M.; Choi, C.H.; Yang, S. *Conjugated Polymers and Aromaticity*, *Chem. Rev.*, **2005**, 105, 3448 - 3481.
44. Na, J.; Kim, Y.; Park, W.H.; Lee, T.S. *Metal-Induced Optical Sensing and Optical Switching in Poly (pyridyl phenylene)*, *J. Polym. Sci. Part A: Polym. Chem.*, **2004**, 42, 2444 – 2450.
45. Lai, L.M.; Lam, J.W.Y.; Tang, B.Z. *Facile Synthesis and High Optical Activity of Poly (1-pentyne) Carrying Amino-Acid Pendant Groups*, *J. Polym. Sci. Part A: Polym. Chem.*, **2006**, 44, 6190 – 6201.
46. Zhang, Y.; Murphy, C.B.; Jones, Jr.; W.E. *Poly [p-(phenyleneethylene)-alt-(thienyleneethylene)] Polymers with Oligopyridine Pendate Groups: Highly sensitive chemosensors for transition metal ions*, *Macromolecule*, **2002**, 35, 630 - 636.
47. Jayakannana, M.; Vanhal, P.A.; Janssen, R.A.J. *Synthesis and Structure-Property Relationship of New Donor–Acceptor Type Conjugated Monomers and Polymers on the Basis of Thiophene and Benzothiadiazole*, *J. Polym. Sci. Part A: Polym. Chem.*, **2002**, 40, 251 - 261.
48. Armbruster, D.A; Tillman, M.D.; Hubbs, L.M. *Limit of Detection/Limit of Quantification Comparison of Empirical and Stastical Methods Exemplified with GC-MS Assays of Abused Drug*, *Clin. Chem.*, **1994**, 40, 1233 - 1238.

Appendices

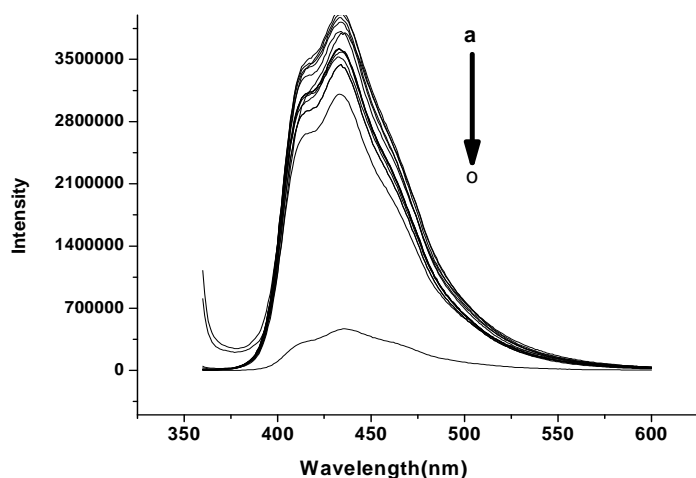
Appendix 1. Absorption spectra recorded for **M1** (6.62×10^{-6} M) and **M2** (6.32×10^{-6} M) in chloroform.



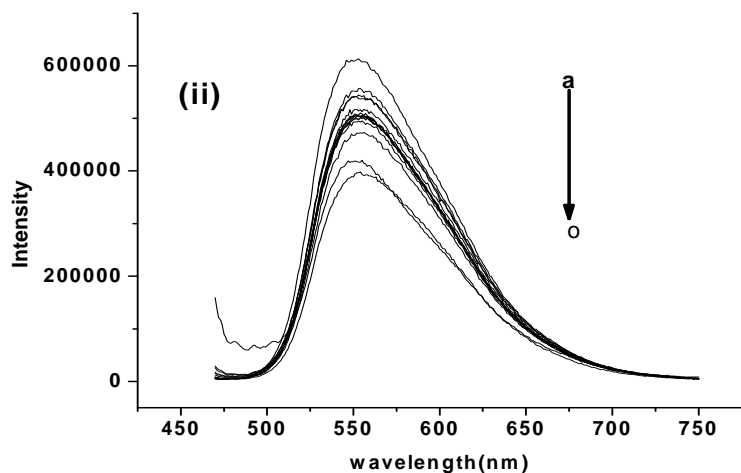
Appendix 2. Fluorescence spectra recorded for monomer **M1** in dioxane upon exposure to different metal ions. Excitation wavelength 350 nm, the concentration of the monomer is 6.62×10^{-6} M and the concentration of metal ions is 1.0×10^{-2} M in methanol.



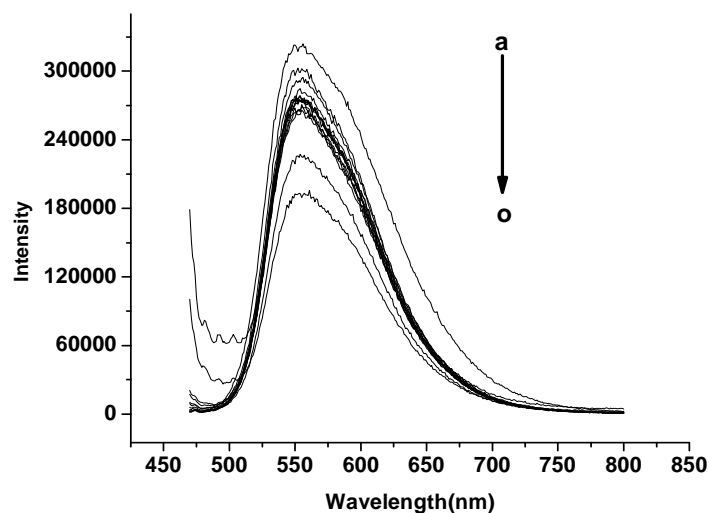
Appendix 3. Fluorescence spectra recorded for monomer **M2** in dioxane upon exposure to different metal ions (a - o; metal free **P1**, Ag^+ , Co^{2+} , Mg^{2+} , K^+ , Ni^{2+} , Hg^+ , Cu^{2+} , Cd^{2+} , Na^+ , Ca^{2+} , Zn^{2+} , Cr^{3+} , Al^{3+} and o. Fe^{3+}). Excitation wavelength 350 nm, the concentration of the monomer is $6.32 \times 10^{-6} \text{ M}$ and the concentration of metal ions is $1.0 \times 10^{-2} \text{ M}$ in methanol.



Appendix 4. Emission spectra for **P1** ($2.3 \times 10^{-7} \text{ M}$) in THF upon addition of $1.0 \times 10^{-2} \text{ M}$ each of metal ions (a – o; metal free **P1**, Ag^+ , Co^{2+} , Mg^{2+} , K^+ , Ni^{2+} , Hg^+ , Cu^{2+} , Cd^{2+} , Na^+ , Ca^{2+} , Zn^{2+} , Cr^{3+} , Al^{3+} and o. Fe^{3+}). Excitation wavelength 348 nm.



Appendix 5. Emission spectra for **P1** (2.3×10^{-7} M) in dioxane upon addition of 1.0×10^{-2} M each of metal ions (a - o; metal free **P1**, Ag^+ , Co^{2+} , Mg^{2+} , K^+ , Ni^{2+} , Hg^+ , Cu^{2+} , Cd^{2+} , Na^+ , Ca^{2+} , Zn^{2+} , Cr^{3+} , Al^{3+} and o. Fe^{3+}). Excitation wavelength 348 nm.



Appendix 6. Solvent polarity parameters [34].

Solvent	Refractive index	$E_T(30)$	Dipole moment
THF	1.406	37.4	1.69
Chloroform	1.438	39.1	1.90
Dioxane	1.422	36.0	0.45
Toluene	0.099	33.9	0.36

Declaration

I, the undersigned, declared that this Msc. Thesis is my original work and has not been presented for any degree in other university and that all sources of materials used have been dully acknowledged.

Name: Wassie Mersha Takele

Signature: _____

This Msc. Thesis has been submitted for examination with my approval as university advisor.

Name: Shimelis Admassie (PhD)

Signature: _____

Place and date of submission: School of Graduate Studies

Department of Chemistry

Addis Ababa University

June 2011